DISSERTATIONS IN

FORESTRY AND NATURAL SCIENCES

ALEXEY ANDRIYASHIN

Non-negative bases in spectral image archiving

PUBLICATIONS OF THE UNIVERSITY OF EASTERN FINLAND

Dissertations in Forestry and Natural Sciences No 49

UNIVERSITY OF EASTERN FINLAND

ALEXEY ANDRIYASHIN

Non-negative bases in spectral image archiving

Publications of the University of Eastern Finland
Dissertations in Forestry and Natural Sciences
No 49

Academic Dissertation
To be presented by permission of the Faculty of Science and Forestry for public examination in the Louhela Auditorium in Joensuu Science Park, on November 25, 2011, at 12 o'clock noon.

School of Computing

Kopijyvä Oy
Joensuu, 2011
Editors: Prof. Pertti Pasanen
Prof. Matti Vornanen, Prof. Kai-Erik Peiponen
Distribution:
Eastern Finland University Library / Sales of publications
P.O.Box 107, FI-80101 Joensuu, Finland
tel. +358-50-3058396
http://www.uef.fi/kirjasto

ISBN: 978-952-61-0567-3, ISSN: 1798-5668 (printed)
ISBN: 978-952-61-0568-0, ISSN: 1798-5676 (PDF)
ISSNL: 1798-5668

Author's address: University of Eastern Finland
School of Computing
P.O.Box 111
80101 JOENSUU
FINLAND
email: alexey.andriyashin@uef.fi

Supervisors: Professor Jussi Parkkinen, Ph.D.
University of Eastern Finland
School of Computing
P.O.Box 111
80101 Joensuu
FINLAND
email: jussi.parkkinen@uef.fi

Professor Timo Jääskeläinen, Ph.D.
University of Eastern Finland
Department of Physics and Mathematics
P.O.Box 111
80101 JOENSUU
FINLAND
email: timo.jaaskelainen@uef.fi

Reviewers: Professor Yoshitsugu Manabe, PhD
Nara Institute of Science and Technology
Graduate School of Information Science
8916-5 Takayama, Ikoma
Nara 630-0192
JAPAN
email: manabe@is.naist.jp

Docent Jorma Laaksonen, Ph.D
Aalto University School of Science
Department of Information and Computer Science
P.O.Box 15400
00076 Aalto
FINLAND
email: jorma.laaksonen@aalto.fi

Opponent: Professor Karen Egiazarian
Department of Signal Processing
Tampere University of Technology
P.O.Box 527
33101 TAMPERE
FINLAND
email: karen.eguiazarian@tut.fi

ABSTRACT:

This thesis supposes an application of Principal Component Analysis (PCA), Non-negative Matrix Factorization (NMF) and Non-negative Tensor Factorization (NTF) for digital image archiving. It is aimed to develop new efficient methods for spectral image acquisition, compression and retrieval. It hypothesizes that the non-negative bases are more suitable for spectral archiving beside convenient orthogonal.
The thesis introduces three fundamental components of the digital image archiving system. It gives an overview of the methods that were developed for the spectral image archiving recently. PCA, NMF and NTF were applied as a spectral reconstruction, a spectral reduction and feature extraction methods. It also supposes a multiresolution approach in computing NTF and subspace clustering preprocessing for compression by PCA.
The experiments performed during the study shows that the non-negative methods reconstruct spectra with the same error but as the benefit they can be implemented optically. The compression method based on subspace clustering is more efficient than convenient k-means. The non-negative basis is better color feature than orthogonal one in a way of spectral image retrieval.

Universal Decimal Classification: 004.93, 519.237.7, 512.643.12,514.743

Keywords (Library of Congress Subject Headings): Image processing, Factor analysis, Calculus of tensors, Matrices

Preface

I would like to express my gratitude to my supervisor, Professor Jussi Parkkinen, whose experience, understanding and support throughout the research helped to my graduate experience. I am thankful to Professor Yoshitsugu Manabe and Docent Jorma Laaksonen, the reviewers of this thesis, for their helpful comments and recommendations.
I owe many thanks to all the staff of Computer Science department and InFotonics Center who make my time at the department comfortable and pleasant. Special thanks to the secretaries Merja Hyttinen and Tanja Karvonen who truly helped me in organization problems.
I am indebted to co-authors of publications, which were published during the research time. Thanks go out to Prof. Timo Jääskeläinen, Dr. Kimiyoshi Miyata, Dr. Arto Kaarna for your support and experience which comes in exact comments and helpful advises.
I wish also to express my gratitude to my university colleagues for providing stimulating and friendly environment. I especially grateful to our director Ph.D. Markku Hauta-Kasari and colleagues Alexey Podlasov, Alexander Kolesnikov, Alexander Akimov, Jukka Antikainen, Jussi Kinnunen, Oili Kohonen, Pesal Koirala, Tuija Jetsu and, of course, Juha Lehtonen for helping me get though the difficult times and enjoy in social activities.
I would like to thank my family for the support and for loving environment they provided me thought my entire life. I am so appreciate my beloved parents, Irina Andriyashina and Alexander Andriyashin for their love and encouragement. Very great thanks go out to my darling wife Anna and daughter Ksenia, who lavish care upon me.

Joensuu November 25, 2011
Alexey Andriyashin

LIST OF ABBREVIATIONS

2D	Two Dimensional
3D	Three Dimensional
CCD	Charge-Coupled Device
CIELAB	CIE 1976 L*a*b*
CMYK	Cyan Magenta Yellow Key
CRT	Cathode Ray Tube
FA	Factor Analysis
GFC	Goodness of Fit Coefficient
GIF	Graphics Interchange Format
GLCM	Gray Level Co-occurrence Matrix
ICA	Independent Component Analysis
IWT	Integer Wavelet Transform
JBIG	Joint Bi-level Image Experts Group
JPEG	Joint Photographic Experts Group
LBP	Local Binary Pattern
LED	Light-emitting Diode
LC	Liquid Crystal
MPEG	Moving Picture Experts Group
MSE	Mean Square Error
NMF	Non-negative Matrix Factorization
NTF	Non-negative Tensor Factorization
PCA	Principal Component Analysis
PGF	Progressive Graphics File
PGP	Prism-Grating-Prism
PNG	Portable Network Graphics
PSNR	Peak Signal-to-Noise Ratio
RGB	Red Green Blue
RMSE	Root Mean Square Error
SOM	Self-Organizing Map
sRGB	Standard RGB
TIFF	Tagged Image File Format
WTA	Winner Take All
XYZ	CIE XYZ

LIST OF SYMBOLS

$\lfloor \cdot \rfloor$	round toward zero
$[\cdot,\cdot]$	horizontal concatenation
$[\cdot,\cdot]^T$	matrix transpose operation
$\lVert\cdot\rVert^2$	square Euclidian norm
$\lVert\cdot\rVert_F^2$	square Frobenius norm
$<\cdot,\cdot>$	inner product
$\otimes$	tensor multiplication
Ø	empty set
a, b, c	corresponding height, width and number of wavelengths
a_{il}	l^{th} approximation element of the i^{th} level wavelet transform
B	color basis for system properties
cr	compression ratio
$c_{\alpha\beta}$	correlation between α^{th} and β^{th} wavelength components
C_S	data correlation matrix or autocorrelation matrix (m×m)
$d_{i,l}$	l^{th} difference element of the i^{th} level wavelet transform
e_i	i^{th} eigenvector
f	camera response value
f_i	scalar camera response for i^{th} filter
f_P	camera response vector for p filters (p×1)
F	camera responses matrix (p×n)
g	high–pass filter in wavelet transform
G	3D non-negative matrix (a×b×c)
h	low-pass filter in wavelet transform
$h(i)$	color histogram
H	non-negative (k×n) matrix of multipliers of NMF
H_{ij}	i^{th} component of j^{th} vector of the H
i, j, μ, ζ, β, α, σ, η	indices

k	transformation rank of PCA, NMF, NTF or clustering number
κ	normalizing factor for XYZ
$l(\lambda)$	light source radiance distribution function
l_i	indexes of clustering, i=[1,…,n]
ℓ	basis of the one dimension subspace L (m×1)
L^*, a^*, b^*	corresponding values of CIE L*a*b*
L_α	basis of the subspace characterizing α^{th} cluster (m×1)
M	number of the color spectra components (wavelengths)
n	number of spectra
n_i	number of pixel with the color equal to i
n_j	number of elements belonging to the j^{th} class
nm	nanometer
N	number of pixels in image
$o(\lambda)$	spectral transmittance function of an optical system
p	filters number
$P(i)$	probability of i^{th} color
$P_s(\ell)$	absolute length of projection of the vector s on vector ℓ
r	spectral reflectance (m×1)
$r(\lambda)$	reflectance power distribution function
$\widetilde{r}$	estimation of a spectral reflectance from camera responses (m×1)
R	reflectance spectra matrix (m×n)
$\hat{s}$	theoretical maximum of the spectrum s
s	color spectrum (m×1)
$s(\lambda)$	spectral power distribution function
$s(\lambda_i)$	i^{th} component of color spectrum
$s^o(\lambda_i)$	i^{th} component of a original spectrum (m×1)
$s^r(\lambda_i)$	i^{th} component of a reconstructed spectrum (m×1)
S	color spectra matrix (m×n)
S^*	reduced spectra (k×n)
S_{ij}	j^{th} component of i^{th} color spectrum of spectra S
S_j	j^{th} color spectrum (m×1) of spectra S

S^R	reconstructed spectra ($m \times n$)
S^α	spectra composed from the samples belonging to the cluster α
$E(S)$	spectral expectation of the spectra S ($m \times 1$)
u	non-negative basis for first domain of NTF ($a \times k$)
u^μ	μ^{th} basis vector of the u basis ($b \times 1$)
u_i^j	i^{th} component of j^{th} basis vector of the u basis
v	non-negative basis for second domain of NTF ($b \times k$)
v^μ	μ^{th} basis vector of the v basis ($a \times 1$)
v_i^j	i^{th} component of j^{th} basis vector of the v basis
w	non-negative basis for third domain of NTF ($c \times k$)
w^μ	μ^{th} basis vector of the w basis ($c \times 1$)
w_i^j	i^{th} component of j^{th} basis vector of the w basis
W	non-negative basis of NMF ($m \times k$) size
W_{ij}	i^{th} component of j^{th} basis vector of the W basis
$\bar{x}(\lambda)$, $\bar{y}(\lambda)$, $\bar{z}(\lambda)$	corresponding CIE XYZ color-matching functions
X_0, Y_0, Z_0	corresponding CIEXYZ values of the reference white point
Y_α	clustering centers
ΔE	color difference
ε_{GFC}	GFC measure
ε_{MSE}	Mean Square Error measure
ε_{PSNR}	PSNR measure
ε_{RMSE}	Root Mean Square Error measure
Θ	pseudo-inverse estimation of Ω
λ	wavelength
σ_i	i^{th} eigenvalues
$\phi(\lambda)$	spectral sensitivity function of the CCD
ω	system properties spectrum
$\omega(\lambda)$	system properties distribution function
$\omega(\lambda_i)$	i^{th} component of system properties
Ω	system properties matrix ($m \times p$)
Ω_k	system properties within k^{th} filter

LIST OF ORIGINAL PUBLICATIONS

This thesis is based on data presented in the following articles:

P1 Lehtonen J., Andriyashin A., Parkkinen J., Leisti T., Nyman G., "Functions of images," *In Proceedings of SPIE, Intelligent Robots and Computer Vision XXIV: Algorithms, Techniques and Active Vision, Vol. 6384*, Boston, Massachusetts, USA, pp. OW-1-OW-10, 2006.

P2 Andriyashin A., Jaaskelainen T., Parkkinen J., Miyata K., "Spectral image compression using clustering and spectral reduction," *In Proceedings of OSAV'08, The 2nd International Topical Meeting on Optical Sensing and Artificial Vision*, Saint-Petersburg, Russia, May 2008.

P3 Kaarna A., Andriyashin A., Nakauchi S., Parkkinen J., "Multiresolution Approach in Computing NTF," *In Proceedings of SCIA 2007, 15th Scandinavian Conference on Image Analysis*, Aalborg, Denmark pp. 333-343, June 2007.

P4 Kaarna A., Andriyashin A., "Comparing sampling methods in faster computation of non-negative tensor factorization of spectral images," *In Proceedings of IEEE IGARSS'08, International Geoscience & Remote Sensing Symposium*, Boston, Massachusetts, U.S.A., pp. III-87 - III-90, July 2008.

P5 Andriyashin A., Kaarna A., "NTF vs. PCA features for searching in a spectral image database," *In Proceedings CGIV 2008/MCS'08, 4th European Conference on Colour in Graphics, Imaging, and Vision, 10th International Symposium on Multispectral Colour Science*, Terrassa-Barcelona, España, pp. 499-504, June 2008.

P6 Andriyashin A., Parkkinen J., Jaaskelainen T., "Illuminant Dependence of PCA, NMF and NTF in Spectral Color

Imaging," *In Proceedings of ICPR 2008, 19th Inter-national Conference on Pattern Recognition*, Tampa, Florida, U.S.A., December 2008.

Throughout the overview, these papers will be referred to as [**P1**]-[**P6**].

Contents

1 Introduction

Digital imaging is an area of computer science where the main role is given to 2D visual information transformed into a binary computer format called digital imaging [1]. It includes such image processes as acquisition, compression, analysis, visualization, printing, etc. The digital image consists of a certain number of elements named pixels; each of them represents a color in the corresponding position. There are several sources from which digital images can be acquired. Usually a digital image originates from a physical scene captured by a camera or scanner device. There light reflected from an object is measured by electronic sensors. The digital image in this case retains the information about the reflected light. Other types of digital images including medical images like Magnetic Resonance Imaging (MRI) [2], Computed Tomography Imaging [3] or X-ray images [4] are based on the property of a substance to transmit and absorb electromagnetic rays. There are also computer generated images using graphical programs, e.g. Photoshop, MathCAD and 3D Studio. They are becoming increasingly popular and closely integrated with natural imaging (e.g. photo-processing, map digitizing and scanning of printed documents). Only digital images taken of natural objects using visible light are considered in this thesis.

The purpose of digital image archives is aimed to store images in an organized order for future use. Images in the archive are protected from external factors (e.g. ageing, corrosion, discoloration). Due to the expansion of digital technologies, the investigation of the physical object can be done quicker and more cheaply using digital image analysis. Also, digital technologies enable transferring a digital image copy over long distances in a short time and representing it in different ways (e.g. paper or textile printing, computer or mobile device representation and light projection) [5].

The most common trichromatic color technologies nowadays, such as RGB (Red Green Blue), are affected e.g. by metamerism (the effect of matching of the color of objects with different spectral power distributions) and are device and observer dependent [6]. Therefore the color spectrum as a discrete analogue of the spectral power distributions is needed for accurate and device independent color representations. An example of color spectra is shown in Figure 1.1.

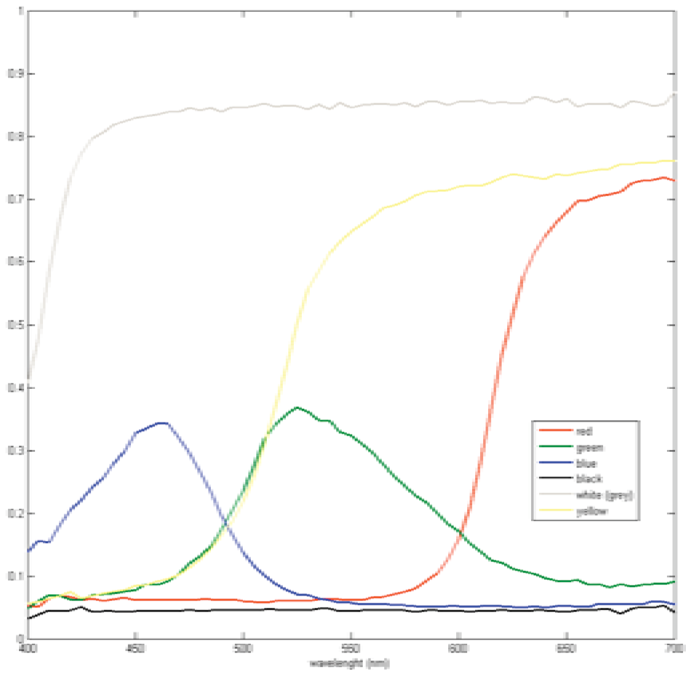

Figure 1.1 *Example of six color spectra represented with corresponding colors. Reflectance spectra of the Macbeth ColorChecker are measured using the PhotoResearch PR-705 spectroradiometer.*

Spectral imaging is an expansion of digital imaging. A spectral image, also called a multispectral or hyperspectral image, is a digital image where each pixel is represented by a color spectrum. From this it follows that the spectral image is an accurate representation of color information. This is deeper and more accurate information than can be captured by mono or three chromatic cameras or visual systems.

Three fundamental processes of the spectral image archive, which are also relevant for any digital image archive, are considered in this study. The processes of acquisition, compression and retrieval are schematically shown in Figure 1.2 and discussed in this thesis. The benefits of spectral color representation compared with trichromatic are explained here. Modern and convenient methods are introduced for each component of the archive. The direction for future research in the area of spectral image archiving is also proposed.

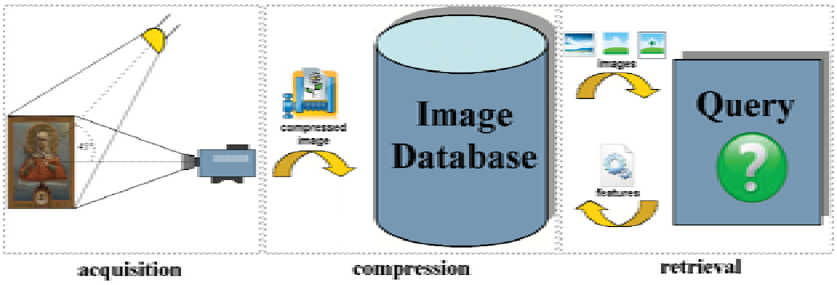

Figure 1.2 Three fundamental components of the digital image archive.

Digital image acquisition is a process of image digitization using an acquisition device e.g. camera or scanner. When the digital image is acquired, it should be stored in a long-term memory. The compression process aims to reduce the amount of allocated memory taken up by the digital image. It allows saving the digital image in a compact format until it is needed. An increasing number of digital images in the archive creates a need for robust methods that can find images in the archive by a relevant query. These methods are called image retrieval.

This dissertation hypothesizes that Principal Component Analysis (PCA) [7], Non-negative Matrix Factorization (NMF) [8] and Non-negative Tensor Factorization (NTF) [9] are suitable for spectral image archiving. These methods were applied to data compression, feature extraction and color spectra reconstruction. The experiments aimed to show the difference between convenient orthogonal bases and non-negative ones.

New approaches to spectral image acquisition, compression and retrieval are proposed and evaluated here.

The dissertation is a compendium of six articles. All of them have appeared in reputable international conferences. The publication [P1] introduces the main aspects of an image database system. A compression method for spectral image archiving was developed in [P2]. The method was successfully applied and compared with another. [P3] provides an acceleration technique for NTF using a multiresolution approach, which is very important since NTF is widely used in our research. The acceleration method was improved in [P4] by subsampling. The publication [P5] gives a new approach to spectral image retrieval. It compares non-negative and orthogonal bases as image color features for database search. An illuminant dependence of PCA, NMF and NTF in the color spectrum domain is investigated in [P6]. It was also shown there that non-negative bases are more suitable for spectral reconstruction.

The dissertation consists of nine chapters. Chapter 1 is an introduction to the study. Digital imaging, color representation and color spectrum representation are explained in Chapter 2. An introduction to the spatial techniques used in all methods developed in this study is presented in Chapter 3. Chapter 4 hypothesizes a new approach to spectral image acquisition systems. Chapter 5 proposes compression methods that are suitable for spectral image archiving. Aspects of retrieval in the spectral image archive system and new features for them are introduced in Chapter 6. A summary of publications can be found in Chapter 7, where my contributions to this study are presented as percentages. Chapter 8 summarizes the result of experiments performed during this study. The conclusions part discusses the main aspects of the study and proposes future work to be done in the area of spectral archive systems.

2 Digital Color Imaging

The definition of color can be given in two ways. First, color is a characteristic of electromagnetic radiation. It means that color sensitivity appears in the brain after the light reflected from an object stimulates eye sensors [10]. It is based on the human visual sensation depended from physical, physiological and psychological factors. This phenomenon is studied in more detail in color symbolism and psychology [11]. From the physical point of view, color is a characteristic of the electromagnetic spectrum taken in the visible range called visible light [12] (see Figure 2.1). It represents the physical properties of the substance to reflect, transmit and radiate light. An individual color sensation depends on the reflectance property of the observed object, the light source spectrum and the individual characteristics of the observer sensors.

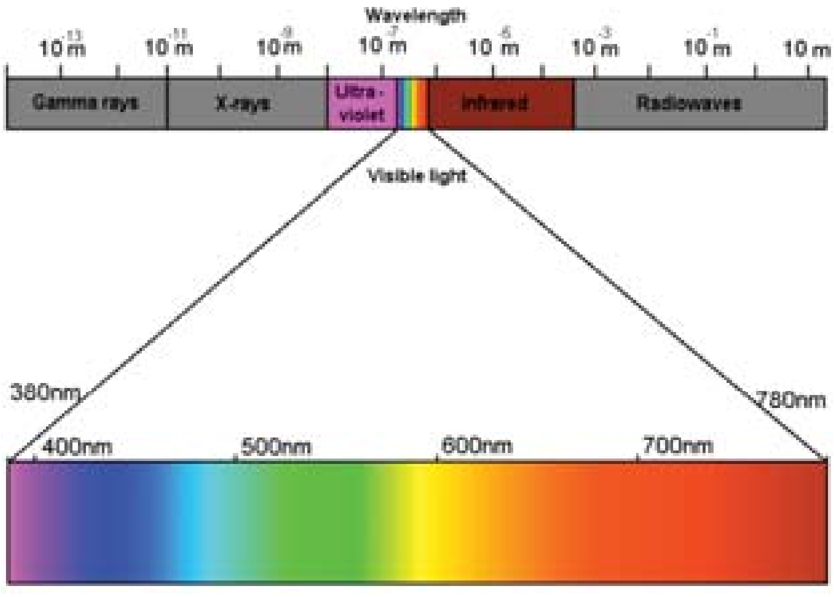

Figure 2.1 *Electromagnetic radiation and visible light.*

2.1 TRICHROMATIC COLOR MODELS

There are many color models (e.g. CIE XYZ, CIE L*a*b*, RGB, CMYK). Most of them are three-dimensional i.e. trichromatic. They are based on three primary colors and arise from the human color vision system consisting of three types of color sensitive photoreceptors called cone cells for short, middle, and long wavelengths [13].

The first trichromatic standard model, defined by the CIE (International Commission on Illumination) in 1931, is XYZ color space (also known as CIE 1931 or CIE XYZ color space) [14]. It was defined based on a series of experiments performed in the late 1920s by W. David Wright [15] and John Guild [16]. As a result of the experiments the color-matching functions $\bar{x}(\lambda)$, $\bar{y}(\lambda)$ and $\bar{z}(\lambda)$ were measured with human observers. They are shown in Figure 2.2 at the visible wavelength range from 380 to 780 *nm*.

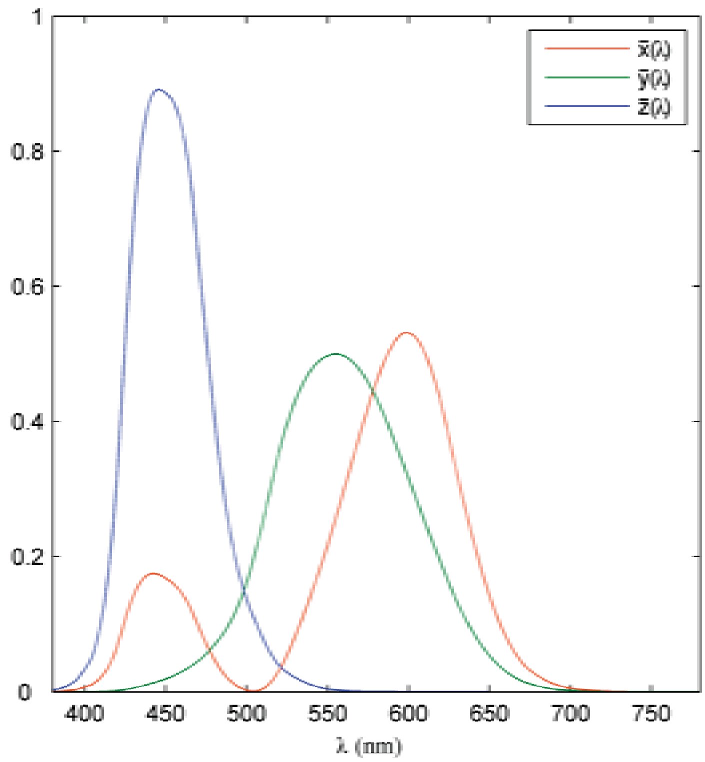

Figure 2.2 *Human color-matching functions* $\bar{x}(\lambda)$, $\bar{y}(\lambda)$ *and* $\bar{z}(\lambda)$.

The corresponding coordinates are calculated over a spectral power distribution $s(\lambda)$ of the reflected light $l(\lambda)$

$$\begin{aligned} X &= \kappa \int s(\lambda)\bar{x}(\lambda)\, d\lambda \\ Y &= \kappa \int s(\lambda)\bar{y}(\lambda)\, d\lambda \\ Z &= \kappa \int s(\lambda)\bar{z}(\lambda)\, d\lambda, \end{aligned} \tag{2.1}$$

where $\bar{x}(\lambda)$, $\bar{y}(\lambda)$ and $\bar{z}(\lambda)$ are color matching functions; $s(\lambda)$ is the product of the light source radiance distribution and the reflectance property of the observed object [17]; and κ is a normalizing factor calculated as

$$\kappa = \frac{100}{\int l(\lambda)\bar{y}(\lambda)\,d\lambda}. \tag{2.2}$$

CIELAB, also known as CIE 1976 L*a*b* uniform color space, was defined by CIE in 1976 [18]. It aimed to linearize color space, which means a change in color value should produce a change of about the same visual importance. This effect is very important to avoid the nonuniformity of color difference. CIE L*a*b* is also a trichromatic color model. *L** indicates the lightness of the color. *a** is a position between green and red (negative values indicate green while positive values indicate magenta). *b** is a position between blue and yellow (negative values indicate blue and positive values indicate yellow). The corresponding CIELAB coordinates are calculated as follows:

$$\begin{aligned} L^* &= 116 f(Y/Y_0) - 16 \\ a^* &= 500 f\left[(X/X_0) - (Y/Y_0)\right] \\ b^* &= 200 f\left[(Y/Y_0) - (Z/Z_0)\right], \end{aligned} \tag{2.3}$$

where

$$f(\alpha) = \begin{cases} \alpha^{1/3} & ,when\ \alpha \geq (6/29)^3 \\ 1/3\,(29/6)^2 \alpha + 4/29 & ,otherwise \end{cases}, \tag{2.4}$$

where X_0, Y_0 and Z_0 are the corresponding CIE XYZ tristimulus values of the reference white point. From this it follows that CIELAB is device and observer independent.

Due to the increasing importance of digital technologies, digital color is becoming more popular. Digital color is a way of numerical representation of color in computer memory. It allows storing, transferring and analyzing color faster and more cheaply than the analog variant.

The best known digital color model is RGB [19]. It is an additive model where colors are an additive combination of the primary red, green and blue. The RGB color model is widely used in computer graphics, e.g. CRT monitors, televisions, video projectors, scanners and digital cameras, although it has two primary problems as well as CIE XYZ. First, RGB is non-uniform color space. The numerical difference between two colors in RGB space is non-linear. The second problem is device-dependency. There are a lot of RGB spaces, and each of them belongs to a corresponding device. The standard sRGB color coordinates under a D65 light source can be calculated over XYZ values by the following formula:

$$\begin{bmatrix} R \\ G \\ B \end{bmatrix} = \begin{pmatrix} 3.241 & -1.5374 & -0.4986 \\ -0.9692 & 1.8760 & 0.0416 \\ 0.0556 & -0.2040 & 1.0570 \end{pmatrix} \begin{bmatrix} X \\ Y \\ Z \end{bmatrix}. \tag{2.5}$$

Due to RGB being one of the simplest color spaces, it is the most popular color space in the digital color area.

2.2 SPECTRAL IMAGING

An electromagnetic spectrum is a discrete analog of a spectral power distribution function. Taken in the visible range of light, the electromagnetic spectrum characterizes a color named the color spectrum. The spectrum is usually represented as an m-dimensional vector $s=[s(\lambda_1),\ldots,s(\lambda_m)]^T$. Here m is the number of color spectra components (number of wavelengths), which depends on the application, e.g. m can be anything from some hundreds to a thousand in remote sensing applications. The visible range from 400 to 700 *nm* with 5 *nm* sampling is accepted as optimal according to Lehtonen et al. [20]. This is the most accurate color representation, and the importance and usage of it is increasing in many areas e.g. medicine, history and quality control.

A spectral image is a digital image where each pixel is described by a color spectrum. It is represented as a 3D matrix in which the first and second dimensions correspond to the image spatial characteristics width and height, and the third one is the spectral domain. A spectral image can be considered either as a set of spectra stored in image pixels or as the set of gray scale images located as wavelength layers. Figure 2.3 a) and b) shows an example of a spectral image and its RGB representation respectively.

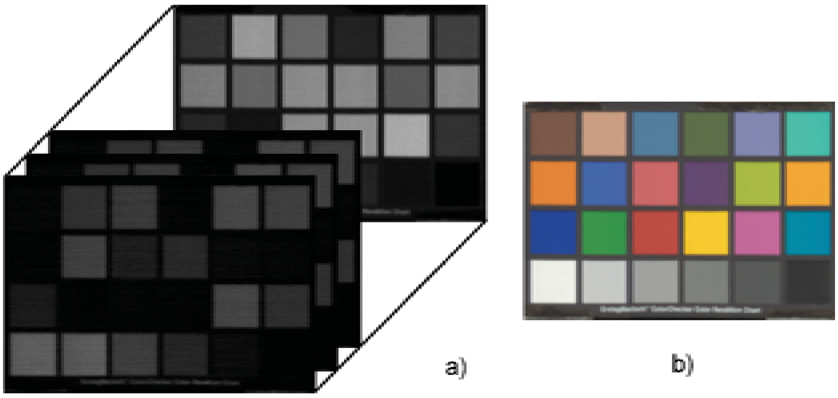

Figure 2.3 *Macbeth ColorChecker: a) 1st 2st, 3st and 61st band; b)RGB representation.*

The increasing use of spectral images has raised questions about the need for a standard spectral image format. Recently, a technical committee of the CIE Division 8, TC8-07 of Multispectral Imaging, has been working to define a general data format for storing spectral images [21]. The reason for this is a problem with data compatibility stemming from the fact that almost all research groups have their own format for storing spectral data and the exchange of spectral images between researchers is not very common at the moment. There are currently five main standards which are widely used in the spectral imaging research area [22].

The MUSP multispectral image file format [23] is a spectral image format developed by Color AIXperts GmbH (Aachen, Germany). All the information necessary to reconstruct the spectra of all pixels is in one file in a simple form. The Natural Vision data file format specification [24] was established in 1999 by the Telecommunications Advancement Organization of Japan (TAO). It aims to enable high-fidelity natural color reproduction in visual telecommunication systems. JPEG2000 [25] is the most recent addition to the family of international standards developed by the Joint Photographic Experts Group (JPEG). TIFF (Tagged Image File Format) [26] is a tag based file format for storing and interchanging raster images. It has spread to video applications, facsimile transmission, medical imaging, satellite imaging as well as document storage and retrieval. HDF5 [27] is a general-purpose library and file format for storing scientific data.

2.3 DIGITAL IMAGE ARCHIVING

Interest in spectral image databases has been increasing over the last years [28] [29]. The increasing importance of spectral image applications is one of the main reasons. Spectral image archive systems and digital image archives in general are mainly based on three main processes, namely acquisition, compression and retrieval. These are represented in Figure 1.2. Many effective techniques have been developed for databases of trichromatic images, but spectral representation of color requires more advanced methods than just managing component images separately, as is commonly done with RGB or similar images. Spectral image databases have been studied in depth by Kohonen et al. [30].

A number of digital image acquisition devices have been developed [31]. Most modern techniques are based on digital photo and video cameras which capture an image in RGB format [32]. The incoming light is separated by filters into three primary colors, and then measured by separate sensors. This technology was patented in 1976 by Bryce Bayer [33] and has been widely improved and applied up until the present day. The main principles of Bayer's filter mosaic are shown in Figure 2.4. Although the first spectral imaging systems were developed in the beginning of the 1970s [34], spectral imaging has not been developed as widely as imaging systems based on RGB images. It was mainly used in the field of remote sensing. However, increasing attention to spectral imaging requires development of a spectral imaging acquisition system in order to obtain spectral images faster and more cheaply.

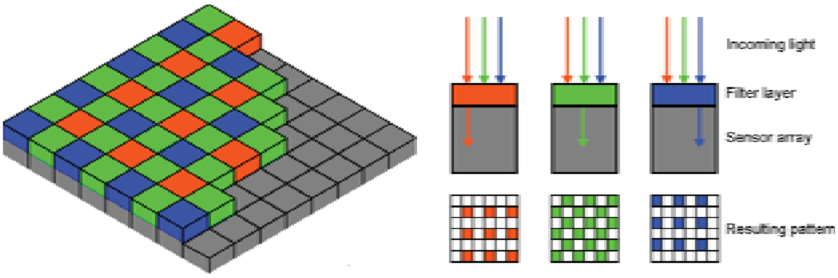

Figure 2.4 *Bayer's filter mosaic principals.*

Image compression is one of the most important tasks in image processing. Applications of image compression are used in such areas as multimedia, data communications, remote sensing, etc. [5]. A common characteristic of all of these applications is that data is too large for them to handle without compression. Images must be small enough for easy management (e.g. transfer, analyses, storage etc.), but the quality of the reconstructed image has to be suitable for further usage. A number of methods have been developed for spectral image compression. Some of them are methods created for trichromatic images, which remove only spatial redundancy (e.g. TIFF [25], JPEG2000 [26], etc.). Others are spectra reduction methods (Principal Component Analysis (PCA) [7], spectrum smoothing [35], subsampling [20], etc.). Such methods as 3D wavelet, Non-negative Tensor Factorization (NTF) [9] and methods which treat the spatial and spectral domain separately belong to the three-dimensional approach. They are the most efficient because they reduce the spatial and spectral domain.

Most of the modern well-known and powerful searching systems (e.g. Google, Yahoo and AltaVista) use text based algorithms even for image retrieval. The queried image is looked for according to the relation between text based features i.e. tags given by the user. Due to an increase in the number of available digital images, more robust image retrieval algorithms based on image content (i.e. texture, shape and color) need to be developed. Most image retrieval algorithms developed nowadays are based on a similarity measurement between content based characteristics of an image [36]. These characteristics are named image features. They are aimed to be much smaller than the original image but characterize the image content as fully as possible. In the spectral imaging area, image features play a big role because spectral images take up a lot of memory and the process of direct comparison between spectral images takes time.

3 Reconstruction Methods

Groups of algorithms, namely PCA, NMF and NTF, are defined in this study as reconstruction methods for spectral image data. The original multidimensional matrix can be reconstructed by them as decomposition of a product of lower dimensional matrixes. These methods and their variants are invaluable tools for blind source separation, feature selection, dimensionality reduction, noise reduction, and data mining [37]. PCA, NMF are methods for two-way representations or two-dimensional reconstruction. Although the original NTF is multidimensional, 3D and 2D approaches are considered in this study. A modification of the 3D NTF aimed to accelerate calculation time has also been proposed.

3.1 PRINCIPAL COMPONENT ANALYSIS

Principal Component Analysis (PCA) [7] is a data transformation technique. In Image Analysis it is usually used when the task is lossy reduction of a large amount of data with high correlation. Suppose there is a set of random spectra $S=[S_1,\ldots,S_n]$, where n is the number of spectra, $S_j=[s(\lambda_1),\ldots,s(\lambda_m)]^T$ is the j^{th} spectrum, and m is the number of wavelengths. The covariance matrix of the spectra set is

$$C_S = \frac{1}{n}\sum_{j=1}^{n}(S_j - E(S))(S_j - E(S))^T \ , \tag{3.1}$$

where spectral expectation $E(S)$ is equal mean spectrum of the spectra set S as

$$E(S) = \frac{1}{n}\sum_{j=1}^{n} S_j \ . \tag{3.2}$$

The components of C_S, denoted by $c_{\alpha\beta}$, represent the correlation between the α^{th} and β^{th} wavelength components of the spectra S. The component $c_{\alpha\alpha}$ is the variance of the α^{th} wavelength component of the spectra S. The variance of a component indicates the spread of the spectrum component wavelength values around its mean value. If two wavelength components e.g. the α^{th} and β^{th} of the spectra S are uncorrelated, their correlation is zero ($c_{\alpha\beta}=c_{\beta\alpha}=0$). The autocorrelation matrix is, by definition, always symmetric. The eigenvectors e_i and the corresponding eigenvalues σ_i of the covariance matrix are the results of the solution of the equation

$$C_S e_i = \sigma_i e_i \ , \tag{3.3}$$

where i=1,…,m corresponds to the number of wavelengths. By putting the eigenvectors in order of descending eigenvalues, an orthogonal basis with the first eigenvectors having the direction of the largest variances of the data can be found. Now the compact form or the reduced spectrum S^* can be found by

$$S^* = [e_1,\ldots,e_k]^T (S - \widehat{S}) \ , \tag{3.4}$$

where k denotes the transformation rank. The reduced spectra S^*, mean spectra $\widehat{S}$ and the basis can be used for spectra reconstruction by

$$S^R = [e_1,\ldots,e_k] S^* + \widehat{S} \ . \tag{3.5}$$

This means that the original spectra S is mean shifted and projected on the coordinate axes having the dimension k and transforming the vector back by a linear combination of the basis vectors. This minimizes the mean-square error between the original spectrum and the reconstructed spectrum using the given number of eigenvectors [38].

If the data is concentrated in a linear subspace, this provides a way to compress data without losing much information and simplifying the representation. By picking the eigenvectors having the largest eigenvalues, as little information as possible is lost in the mean-square error sense [38]. One can e.g. choose a fixed number of eigenvectors and their respective eigenvalues and get a consistent representation or an abstraction of the spectra. This preserves a varying amount of information of the original spectra. Alternatively, we can choose approximately the same amount of information and a varying amount of eigenvectors and their respective eigenvalues. This would in turn give an approximately consistent amount of information at the expense of varying representations with regard to the dimension of the subspace.

3.2 NON-NEGATIVE MATRIX FACTORIZATION

Non-negative Matrix Factorization (NMF) has been widely used in image processing [8] [39] [40] [41] [42]. It solves the factorization problem by finding non-negative matrix factors *W* and *H* of the original matrix *S* as

$$S \approx WH \tag{3.6}$$

where the original data *S* is approximated by two non-negative matrices: *W* of size ($m \times k$) and the matrix *H* of size ($k \times n$), hence the *S* of size ($m \times n$). The main term of the NMF problem is that both parts of the equation (3.5) consist of non-negative elements. To find an approximate factorization a cost function that quantifies the quality of the approximation is defined as Euclidean distance. NMF is based on the minimization of the cost function

$$\min_{W,H \geq 0} \left\| S - WH \right\|_F^2 , \tag{3.7}$$

where $\|.\|_F^2$ is the square Frobenius norm, i.e. the sum of squares of all entries elements. From this description, a reduced representation is achieved by choosing rank k. Solutions to the minimization problem (3.7) have been found using gradient descent. In NMF the following iterative learning rules are used to find linear decomposition [42]:

$$H_{\alpha\eta} \leftarrow H_{\alpha\eta} \sum_{i=1}^{m} W_{i\alpha} \frac{S_{i\eta}}{(WH)_{i\eta}}, \tag{3.8}$$

$$W_{\mu\alpha} \leftarrow W_{\mu\alpha} \sum_{j=1}^{n} \frac{S_{\mu j}}{(WH)_{\mu j}} H_{\alpha j}, \tag{3.9}$$

$$W_{\mu\alpha} \leftarrow \frac{W_{\mu\alpha}}{\sum_{i=1}^{m} W_{i\alpha}}, \tag{3.10}$$

where α=1,…,k, μ=1,…,m and η=1,…,n. The initial value of W and H is random. The output from the optimization problem is matrixes W and H.

The factorization rank k can be varied by the user depending on the application. The normal restriction is that the number of samples in S is larger than the sum of samples in W and H, i.e. $(n+m)k<nm$. The factorization process is schematically presented in Figure 3.1.

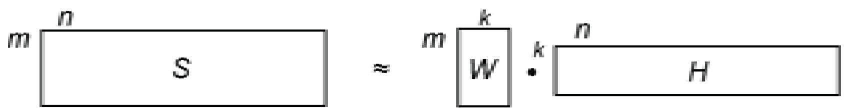

Figure 3.1 *Non-negative matrix factorization.*

3.3 3D NON-NEGATIVE TENSOR FACTORIZATION

3D Non-negative Tensor Factorization (3D NTF) [9] [43] [44] finds the reconstruction of original data as a sum of three vectors multiplied by tensor product

$$G \approx \sum_{\mu=1}^{k} u^{\mu} \otimes v^{\mu} \otimes w^{\mu} , \tag{3.11}$$

where G is the original 3D non-negative matrix with (a×b×c) size, $\otimes$ is a tensor multiplication, a-dimensional vectors u^{μ} from the basis for the first domain of the matrix G, b-dimensional vectors v^{μ} from the basis for the second domain of G, and c-dimensional vectors w^{μ} from the basis for the third domain. All elements of u^{μ}, v^{μ} and w^{μ} are non-negative, k is the factorization rank, and a normal requirement is $(a+b+c)k<a\cdot b\cdot c$. The factorization process is schematically presented in Figure 3.2.

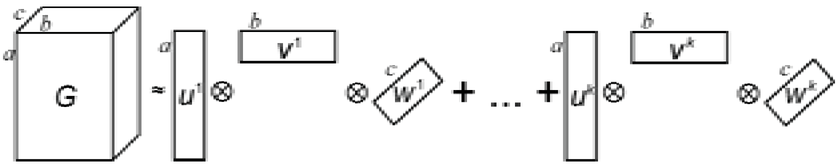

Figure 3.2 *Non-negative tensor factorization for 3D data.*

The basic approach of NTF is to find a solution to the problem

$$\min_{u^{\mu}, v^{\mu}, w^{\mu} \geq 0} \left\| G - \sum_{\mu=1}^{k} u^{\mu} \otimes v^{\mu} \otimes w^{\mu} \right\|_F^2 , \tag{3.12}$$

where $\|\cdot\|_F^2$ is the square Frobenius norm. A multiplicative update rule for the NTF minimization problem (3.12) is given in [9]. The approach minimizes the reconstruction error in the Frobenius norm sense. The iteration steps for u, v and w are respectively defined as

$$u_i^j \leftarrow \frac{u_i^j \sum_{\beta,\zeta} G_{i,\beta,\zeta} v_\beta^j w_\zeta^j}{\sum_{\mu=1}^k u_i^\mu < v^\mu, v^j >< w^\mu, w^j >}, \quad i=1,...,a,\ j=1,...,k\,, \quad (3.13)$$

$$v_i^j \leftarrow \frac{v_i^j \sum_{\alpha,\zeta} G_{\alpha,i,\zeta} u_\alpha^j w_\zeta^j}{\sum_{\mu=1}^k v_i^\mu < u^\mu, u^j >< w^\mu, w^j >}, \quad i=1,...,b,\ j=1,...,k\,, \quad (3.14)$$

$$w_i^j \leftarrow \frac{w_i^j \sum_{\alpha,\beta} G_{\alpha,\beta,i} u_\alpha^j v_\beta^j}{\sum_{\mu=1}^k w_i^\mu < u^\mu, u^j >< v^\mu, v^j >}, \quad i=1,...,c,\ j=1,...,k\,, \quad (3.15)$$

where <.,.> refers to the inner product and α=1,…,a, β=1,…,b, ζ=1,…,c. Note that the update rule preserves non-negativity provided that the initial values for the vectors u, v, w are non-negative. In any iteration of the update process, the values of u^j are updated Jacobi style with respect to the entries u_i^j for i=1,…,a and are updated Gauss-Seidel style with respect to the entries of other vectors $\{u^\mu\}\mu \neq j$ and vectors $\{v^\mu, w^\mu\}_{\mu=1}^k$. The general convergence proof of the multiplicative rule was introduced in [43] for the bilinear case. The main difference is that the NTF update rule is performed in a Gauss-Seidel fashion for the vectors u^1,..., u^k while their update rule is performed Jacobi style. Since a Jacobi-type update rule is used only for a single vector u^j the optimization function with respect to the variable u_i^j has a diagonal Hessian matrix – the proof of this is in [9].

3.4 2D NON-NEGATIVE TENSOR FACTORIZATION

2D NTF can be defined by neglecting one of the domains in the 3D approach (3.11). Since the spectra data set S is only two-dimensional, the first domain is the spectral domain (m-size) and the second domain consists of the large number of spectra

n. Now the solution of the optimization problem (3.12) can be represented as

$$\min_{u,v\geq 0}\left\|S-uv^{T}\right\|, \tag{3.16}$$

where the original 2D data S is approximated by two non-negative matrices: u of size (m×k) and the matrix v of size (n×k), hence the S of size (m×n). A multiplicative update rule for the NTF minimization problem (3.13-14) can be modified for the 2D approach. The iteration step is defined as follows:

$$u_i^j \leftarrow \frac{u_i^j \sum_{\eta=1}^{n} S_{i,\eta} v_\eta^j}{\sum_{\mu=1}^{k} u_i^\mu < v^\mu, v^j >}, \tag{3.17}$$

where i=1,…,m, j=1,…,k,

$$v_i^j \leftarrow \frac{v_i^j \sum_{\eta=1}^{m} S_{\eta,i} u_\eta^j}{\sum_{\mu=1}^{k} v_i^\mu < u^\mu, u^j >}, \tag{3.18}$$

where i=1,…,n, j=1,…,k and <.,.> refers to the inner product.

3.5 INTEGER WAVELET TRANSFORM

The wavelet transform performs the appropriate approximation of the data [45]. The original data is transformed to the approximatve component and to the detail component. In the inverse wavelet transform these two components are used to reconstruct the data. The wavelet transform carries the perfect reconstruction property [46]. The principle of multiresolution is illustrated in Figure 3.3, a), b). The lower level approximation is received as values a_{j+1} from the original values a_j. In practice the transform is performed using convolution with low-pass filter h and high-pass filter g. Different requirements can be set when defining the filters [46].

The wavelet transform is one-dimensional in nature. In an image that is a two-dimensional signal, the one-dimensional transform is applied to the rows and columns of the image. In the three-dimensional case, the one-dimensional transform is applied to all dimensions separately. The principle of the three-dimensional, separable transform is shown in Figure 3.3, c).

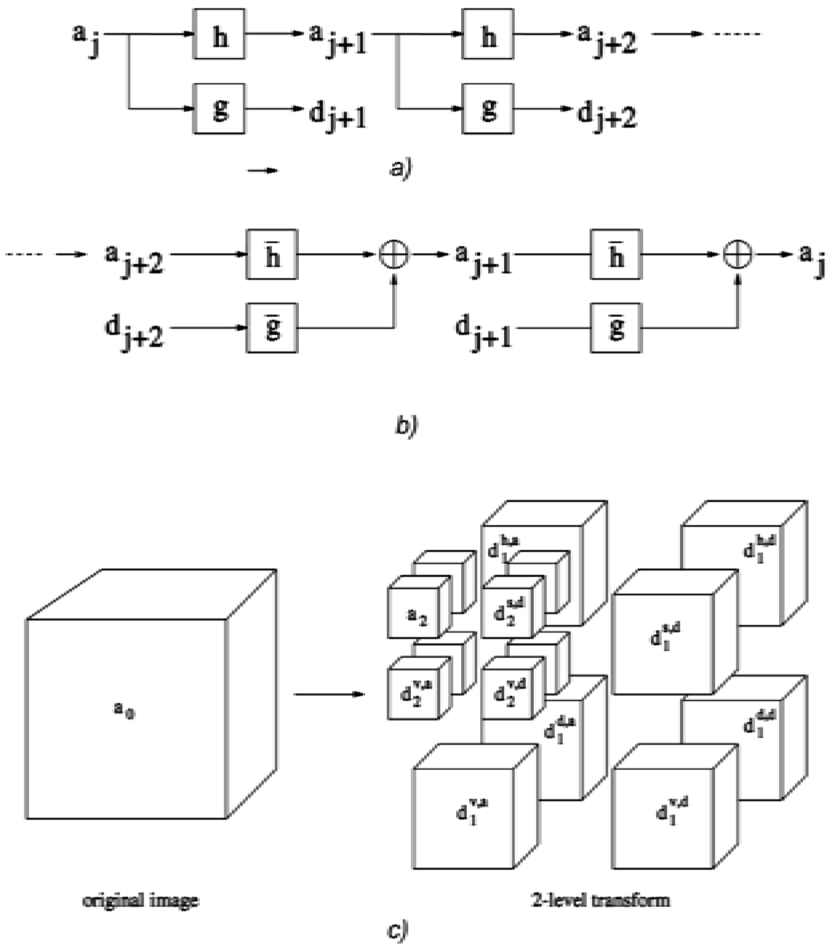

__Figure 3.3__ Wavelet transform. a) Forward transform. b) Inverse transform, c) Separable three-dimensional wavelet transform applied twice [P3].

One of the simplest and best known wavelet transforms is the Integer Wavelet Transform (IWT), which is based on the Haar discrete transform [47]. This transform is used in the study. The basic form of the IWT on the j^{th} level subtracts even samples from odd samples to get the difference d_{j+1} and the new approximation a_{j+1} as

$$d_{j+1,l} = a_{j,2l+1} - a_{j,2l}, \quad a_{j+1,l} = a_{j,2l} + \lfloor d_{j+1,l}/2 \rfloor, \tag{3.19}$$

where the original data is stored in a_j. The second subscript refers to the index in the sample vector. The exact reconstruction comes from calculating the values in reverse order as

$$a_{j,2l} = a_{j+1,l} - \lfloor d_{j+1,l}/2 \rfloor, \quad a_{j,2l+1} = a_{j,2l} + d_{j+1,l}\,. \tag{3.20}$$

3.6 MULTIRESOLUTION NON-NEGATIVE TENSOR FACTORIZATION

NTF algorithm convergence is slow because the process is iterative and initialization is random. The multiresolution approach, which is aims to accelerate algorithm convergence, is proposed in [P3] and investigated in [P4]. It is based on an approximation of the original data by wavelet transform. The original data is transformed to the approximative component and to the detail components. In the inverse wavelet transform these components are used to reconstruct the data. The wavelet transform carries the perfect reconstruction property.

Finally, the multiresolution approach to NTF computation consists of the following steps:

Algorithm 3.1:

Begin

Compute the lowest resolution transform using (3.19) for the original data set.

Compute u, v, and w (Eqs. 3.13, 3.14, 3.15) for this lowest level in multiresolution.

repeat

Interpolate u, v, and w for the next higher level in multiresolution.

Use (3.20) to compute the next higher level in multiresolution.

Compute u, v, and w for the current multiresolution level.

until u, v, and w are computed for the highest level in multiresolution.

End

The number of iterations depends on the data set used in the application. Typically, hundreds or even thousands of iterations are needed for the process to converge. We suppose the criteria of the iteration converge is a limit of the average similarity measure between the bases u, v, w and the corresponding bases obtained in the previous iteration.

3.7 ERROR AND QUALITY MEASURES

Reconstruction methods, which are the primary objects of consideration in this study, are evaluated by numerical characteristics [48] [48]. They are mainly separated into two groups. The first group of characteristics characterizes compression method efficiency e.g. the compression ratio. The second group represents the information loss e.g. peak signal-to-noise ratio (PSNR) [50] and goodness of fit coefficient (GFC) [51], ΔE [12].

Compression ratio cr [52] represents a ratio between the number of bits of the original and the compressed images. It is calculated as

$$cr = \frac{\text{number of bits for the original image}}{\text{number of bits for the compressed image}}. \tag{3.21}$$

The compression losses can be evaluated by quality and error measures. They are all based on the mean pixelwise reconstruction accuracy and calculated between original and reconstructed spectra as mean value over the image.

Two of the most convenient error measures were used in our study. The color difference ΔE between two colors in CIE L*a*b* color space is the standard color quality measure. It is defined as

$$\Delta E = \sqrt{\Delta L^{*2} + \Delta a^{*2} + \Delta b^{*2}}\ , \tag{3.22}$$

where ΔL^*, Δa^* and Δb^* are differences between the corresponding CIE L*a*b* coordinates.

Root mean square error (RMSE), from spectral point of view, is the Euclidean distance [53] between an original and a reconstructed spectrum divided into square toot of the dimension of the spectrum (number of wavelengths). The error measure, which originally is Euclidean distance, is used in this study and defined as

$$\varepsilon_{RMSE} = \sqrt{\sum_{i=1}^{m} \left(s^o(\lambda_i) - s^r(\lambda_i)\right)^2}\ , \tag{3.23}$$

where $s^o(\lambda_i)$ and $s^r(\lambda_i)$ are components of the original and reconstructed color spectrum, correspondingly. m is the number of wavelengths.

The quality measures and RMSE are based on the average pixelwise difference between an image's spectrums. As opposed to error, quality measures become higher when the evaluated spectra are similar. The quality measures are represented in this study by the goodness of fit coefficient (GFC) and peak signal-to-noise ratio (PSNR).

GFC [49] between two spectra is calculated as

$$\varepsilon_{GFC} = \frac{\sum_{i=1}^{m} s^o(\lambda_i) s^r(\lambda_i)}{\sqrt{\sum_{i=1}^{m} s^o(\lambda_i)^2 \sum_{i=1}^{m} s^r(\lambda_i)^2}}, \tag{3.24}$$

where $s^o(\lambda_i)$ and $s^r(\lambda_i)$ are components of the original and reconstructed color spectrum, correspondingly. m is the number of wavelengths.

PSNR is a quality measure expressed in decibels (dB). It represents the computational quality of the spectra. PSNR is defined as

$$\varepsilon_{PSNR} = 10\log_{10} \frac{\hat{s}^2}{\varepsilon_{MSE}}, \tag{3.25}$$

where $\hat{s}$ is the theoretical maximum of the spectrum and ε_{MSE} is the mean square error between the original and reconstructed spectra calculated as

$$\varepsilon_{MSE} = \frac{1}{m} \sum_{i=1}^{m} \left(s^o(\lambda_i) - s^r(\lambda_i) \right)^2, \tag{3.26}$$

where $s^o(\lambda_i)$ and $s^r(\lambda_i)$ are components of the original and reconstructed color spectrum, correspondingly. m is the number of wavelengths.

4 Image Acquisition

From silver halide photography to modern highly accurate digital cameras, the acquisition process has been the most important part of image processing [34]. Most of the modern image acquisition devices sense light reflected from the object and transform it into a digital format. The quality of the acquired image mostly depends on such aspects as illumination, camera optics and sensors. The increasing importance of digital imaging has created a need to develop new cheaper, quicker and more accurate spectral image acquisition systems.

This chapter introduces spectral image acquisition systems. Three of the best known approaches, namely dispersive, narrowband and spectra reconstruction, are presented here. This section also presents a spectral image acquisition system which is based on light source simulation [54]. In this study, a new way to design the light source using a statistical approach to NTF is described. The image is reconstructed from the acquired NTF data.

4.1 NARROW BAND FILTERS BASED CAMERAS

There have been several implementations of spectral cameras using narrow-band interference filters [55]. Figure 4.1 shows the main working principle of these cameras. The system consists of a set of interference filters which are attached to a rotating tablet. Component images are acquired one by one by a monochromatic charge-coupled device (CCD) camera as regular gray-scale images through narrow band interference filters. The spectrum of the light source must be measured beforehand. Using this spectral image acquisition system, color reproduction with high accuracy and illumination difference correction is possible. However, the measured object should stay stable during scanning. The accuracy of the camera mostly depends on the number of filters and shape of the color spectrum of each filter. The filter must be designed so that the intersection of the color spectrums is as small as possible.

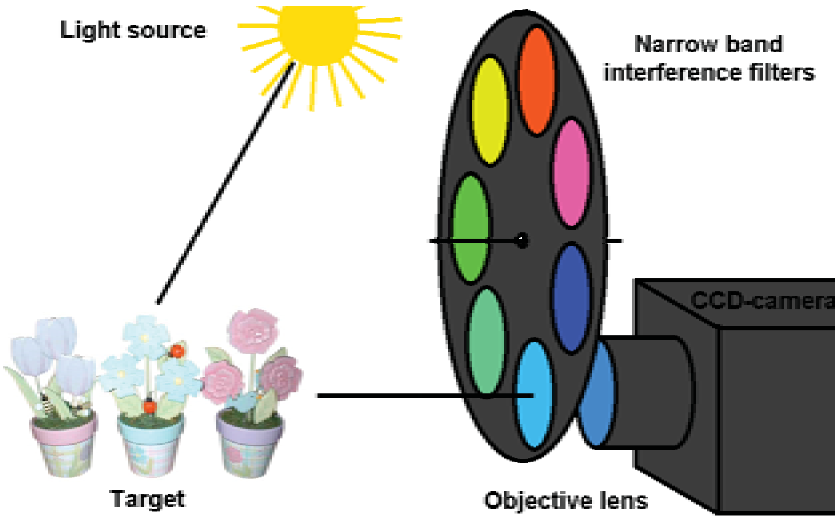

Figure 4.1 *The narrow band interference filter based spectral image acquisition system.*

4.2 PRISM-GRATING-PRISM BASED CAMERAS

A property of the electromagnetic waves to refract in a prism with a different bending degree is utilized into line-scan imaging spectrograph. A light, passing through prism-grating-prism (PGP) element, is broken up into its constituent spectral colors. Short wavelength rays are refracted with higher dispersion than long ones. It allows measuring a spectral power distribution of the light for every wavelength with the certain accuracy.

The principle a line-scan imaging spectrograph is shown in Figure 4.2. The reflected from the object light is passed through a horizontal slit, holding the information of the one selected sampling line. Vertical dimension of a sensor matrix in PGP cameras is reserved for wavelength measurement. Passed thought PGP element light is reflected into the light sensor. The spectral power distribution for each pixel in the sampling line is measured along the vertical direction [56].

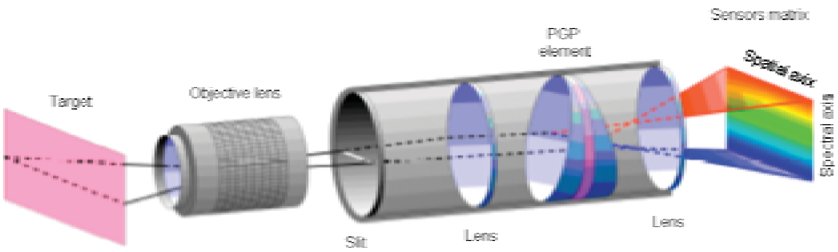

Figure 4.2 *The PGP based spectral image acquisition system [56].*

To digitize an entire object the image must be built up line by line. It requires a relative movement between the sample and the spectrograph. This is usually achieved by mechanically scanning the object past the slit. Once the scanning operation is finished, the system has acquired a series of images each with one spatial and one spectral axis. For the following data evaluation, it is convenient to treat these images as a three-dimensional data set with two spatial dimensions and one spectral axis. Following this methodology, it is the most suitable to acquire spectral images small objects and of flat surfaces e.g. paper or textile.

4.3 SPECTRUM REPRODUCTION APPROACH

The reflectance spectra of natural objects and printed media having relatively low dimensionality [57]. Moreover, it has been shown that the color spectra can be reproduced accurately from the low-dimension representation of spectra [58]. In recent years, various imaging systems with color reproduction have been developed basing of the reconstruction property of color spectra [59].

It was proposed a multichannel vision system which is based on the use of a CCD camera and six color filters in 1996 by Tominaga [60] [59]. More advance multispectral imaging system with 29 filters in a wavelength range from 420 nm to 1550 nm was built by Baroni et al. later on [61]. Haneishi et al. [62] has used a five-color acquisition system for spectral image archiving. Optimization an energy function based on second and fourth order statistical moments allows Lenz et al. to design an unsupervised low-dimensional color filter set [63].

The main components of the image acquisition system are represented in Figure 4.3. The spectral radiance of the light source is denoted as $l(\lambda)$, the spectral reflectance of the measured object as $r(\lambda)$, the spectral transmittance of an optical system including a color filter as $o(\lambda)$ and the spectral sensitivity of the CCD array as $\phi(\lambda)$.

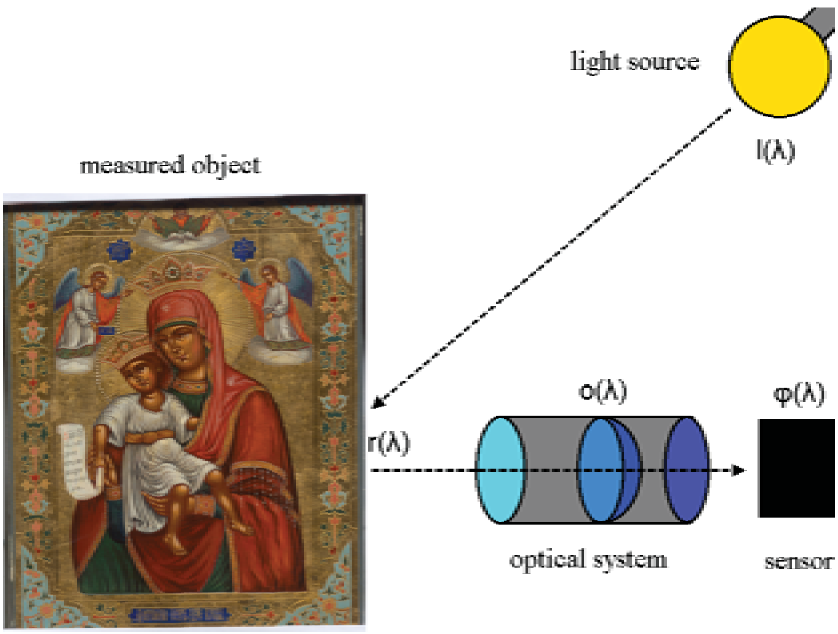

Figure 4.3 *Schematic view of the image acquisition system.*

The camera response f in scalar form is calculated as [64]

$$f = \int_{\lambda_{\min}}^{\lambda_{\max}} \omega(\lambda) r(\lambda) d\lambda \,, \tag{4.1}$$

where $r(\lambda)$ is the object reflectance spectrum and $\omega(\lambda)$ is the system properties denoted by

$$\omega(\lambda)=l(\lambda)o(\lambda)\phi(\lambda). \tag{4.2}$$

For discrete convenience, the camera response equation (4.1) can be rewritten as a scalar product

$$f=\omega^T r, \tag{4.3}$$

where $r=[r(\lambda_1),\dots,r(\lambda_m)]^T$ is the object reflectance spectrum and $\omega=[\omega(\lambda_1),\dots,\omega(\lambda_m)]^T$ is the system property in uniformly sampling at an m wavelength interval.

Direct measurements of the reflectance with monochromatic light require expensive equipment. We suppose the popular indirect approach where the camera responses $f_P=[f_1,\dots,f_p]^T$ to an unknown reflectance r, using a set of p chromatic filters or illuminants with known spectral characteristics, may be described as [65]

$$f_P=\Omega^T r, \tag{4.4}$$

where $\Omega=[\Omega_1,\dots, \Omega_p]$ is an $(m\times p)$ matrix of system properties within p filters or light conditions. $f_P=[f_1,\dots,f_p]^T$ represents the camera responses to unknown reflectance $r=[r(\lambda_1),\dots,r(\lambda_m)]^T$.

The problem of estimating a spectral reflectance $\tilde{r}$ from the camera responses f_P for system Ω is usually formulated as finding an estimation Θ that reconstructs the spectra from the measurement vector

$$\tilde{r}=\Theta f_P, \tag{4.5}$$

where Θ is an $(m\times p)$ matrix. Three approaches are commonly used to find Θ by using spectral reflectance of n samples of a training set $R=[r_1,\dots,r_n]$ and corresponding camera responses $f_P=[f_1,\dots,f_p]^T$: the method based on PCA [66], the method based on Wiener estimation [67], and the methods using multiple regression approximation [68].

4.4 PROPOSED ESTIMATION METHOD

The spectral reflectance of the training set R is approximated as follows:

$$R=WH, \tag{4.6}$$

where R is a ($m \times n$) matrix of the measured sample reflectance spectra, W ($m \times k$) is the spectral basis and H is a ($k \times n$) matrix of multipliers. The spectral camera response given by (4.4) can be represented for R spectra as

$$F=\Omega^T WH, \tag{4.7}$$

where F is an ($p \times n$) matrix of the camera responses n color samples measured within p filters or light conditions. The matrix of multipliers H is denoted as follows:

$$H=(\Omega^T W)^{-1}F. \tag{4.8}$$

Using (4.6) and (4.8) the approximation of R follows as

$$R=W(\Omega^T W)^{-1}F. \tag{4.9}$$

Considering (4.5) for approach of training set R and measured camera responses F, the estimation of Θ can be calculated as:

$$\Theta=W(\Omega^T W)^{-1}, \tag{4.10}$$

where W is the color basis for system properties Ω.

The basis vector set for any spectral set calculated by PCA is orthogonal and contains negative coefficients. This disadvantage makes measurement more complicated. First, the object is illuminated by spectral power distribution consisting of positive elements and then negative. Kaarna et al. [69] showed that a non-negative basis for various spectral color sets can be found by NMF. In [P6] it was proved that non-negative methods, e.g. NMF and 2D NTF, have approximately the same reconstruction error compared with PCA for different spectral sets under different light sources.

Assuming that the rank of the factorization k can be chosen as any and, due to non-negativity, the color basis W can be implemented optically, the estimated spectra is as follows:

$$\widetilde{r} = W(\Omega^T W)^{-1} f_P \tag{4.11}$$

A future task is to implement the calculated color bases optically, construct the measurement system with implemented color filters and check the feasibility of the proposed technique experimentally.

The following presents examples of two novel spectral color acquisition systems based on color reconstruction. The main idea of them is to perform color measurement by a standard CCD camera under different light sources, where the spectrum of light sources is produced by subspace methods [54] [70].

4.4.1 Computer Controlled Set of Light-emitting Diodes

Parkkinen et al. [58] showed that a spectral database containing 1257 samples measured from the Munsell book of colors [71] can be represented accurately by a few basis vectors produced using a subspace method. Principal Component Analysis allows finding an optimal (low-dimensional) set of basic spectra with which any natural color spectrum can be reconstructed with any required precision. The spectral color acquisition system was built [54] based on this fact. It consists of a set of light-emitting diodes and generates any predefined basic spectrum with the possibility of fast switching from one spectrum to another.

The Nippolainen and Kamshilin [54] system is presented inFigure 4.4. It consists of a set of LEDs which generates light at different wavelengths and covers the whole visible range. Emitted by the LED set, light travels through collimators to the diffractive grating, where it is mixed and directed to the same angle. In addition, a slit is used to control the bandwidth of the outline spectral lines. The electronic unit of the light source was designed to provide the injection current of LEDs and the width of the slit. Thus an operator may form color vectors, which are different sequences of spectral lines with different output power.

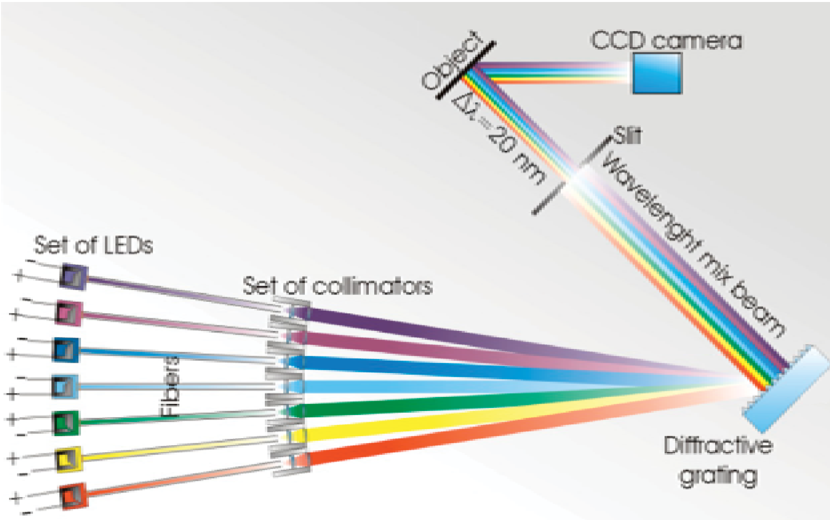

Figure 4.4 *Optical setup for the Computer Controlled Set of Light-emitting Diodes [54].*

4.4.2 Liquid Crystal Spatial Light Synthesizer

Hauta-Kasari et al. [70] designed a low-dimensional color filter set for the 1269 Munsel spectra using a supervised neural network. The competitive learning algorithm was based on the Instar–algorithm by Grossberg [72], which was introduced by Kohonen's [73] self-organizing map with the winner take all (WTA) layer. The natural network clusters of the color spectra and, after learning, the centers of the clusters are used as color filters. Detailed descriptions of competitive learning and self-organization can be found in [72] [73], and [74]. It was shown in [70] that the Munsell spectral set was reconstructed by the designed color filters with sufficient accuracy and the reconstruction accuracy was comparable to the subspace method.

It was implemented optically using the Liquid Crystal Spatial Light Synthesizer. The white light source is a halogen lamp pair. The light is introduced to a narrow slit by a fiber light guide and then reflected by a mirror and incident on a concave grating. The collimated light is dispersed on the focal plane of the concave grating. On the dispersion plane there are a rectangular window, a cylindrical lens and liquid crystal (LC) panel. The transmittance of the LC panel along the wavelength axis is controlled by a computer through a monochrome image board and LC driver. The light passing through the LC panel is finally mixed by a second concave grating. The function of the cylindrical lens in the dispersion plane is to gather light energy effectively into the second grating in order to prove good mixing and to make the light loss as small as possible. Mixed light from the second grating is directed to the measuring plane by a mirror. The schematic representation of the optical setup for the spectral synthesizer is shown in Figure 4.5 (modified from [70]).

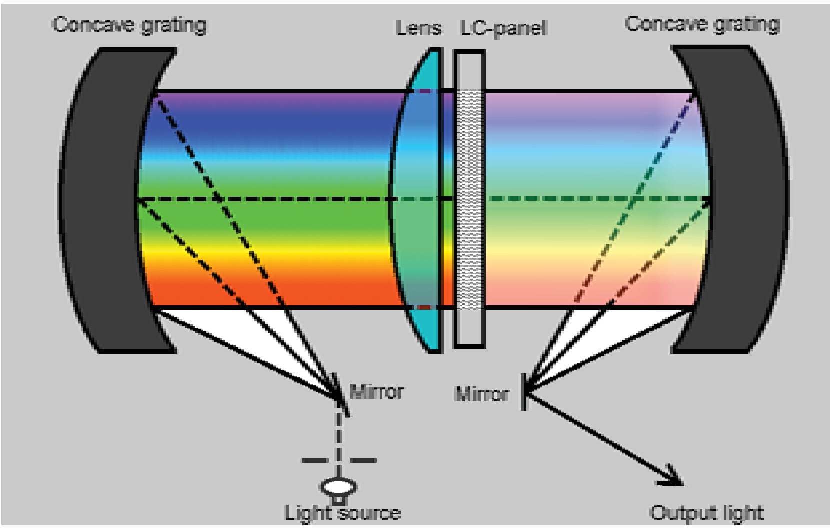

Figure 4.5 *Optical setup for the Liquid Crystal Spatial Light Synthesizer [70].*

Comparing the methods introduced above we can conclude that the measurement system based on liquid crystals is more accurate. It simulates a color spectrum by using diffracted light. Since there are no mechanical elements, the system is fast and reliable. The benefit of the LED system is price as Light-emitting Diodes are becoming cheaper.

5 Compression

Image compression is an important task in digital imaging. Memory expense and the fact that most digital images take more storage memory in an original than in a compressed format have created a need to develop efficient compression methods. Most compression methods are based on reduction of data redundancy, e.g. the number of image pixels with the same color value in digital imaging. These values can be coded by short binary sequences.

Image compression is widely used in such areas as multimedia, image archives, data communication and remote sensing. A number of image compression methods have been developed in recent years [52]. They are mainly defined as lossy or lossless compression [5]. Lossless image compression (e.g. PNG, TIFF, GIF) [75] is performed in images with high value content e.g. medical imaging. The original image can be reconstructed after compression by decompression. Images with high content prediction or high redundancy are compressed by lossy compression methods such as JPEG, JBIG and PGF [25]. These compression methods reconstruct the original image data with small losses. The benefit of lossy methods comparing with lossless is the significant difference in size between the original and compressed files.

Most of the image compression methods developed in the past are suitable for gray-level or RGB images. Due to the increasing importance of spectral imaging, we need compression methods with more advantages than managing an image's layers separately, as is commonly done with trichromatic images. A number of methods have been developed recently [76] [77] [78] [79]. Some of them are methods that treat the spatial and spectral domain separately. An example of this is an approach including combinations like 2D wavelets in the spatial domain and principal component analysis (PCA) in the spectral domain [80] [81]. Methods assuming the 3D property of the spectral image, e.g. 3D wavelets [82] and NTF [43], are also used in the area of spectral imaging.

5.1 CLUSTERING METHODS

Clustering is a set of unsupervised pattern recognition methods, which are aimed at separating a data set into a number of subsets (clusters) characterized by a clustering table or clustering centers [83]. The process of finding the final values of the clustering centers is usually iterative. At each step the input data is split into a number of clusters and the center of each cluster is adjusted by minimizing the scheme of an associated performance index which replaces the cluster center by the arithmetic mean of the cluster's samples. The process terminates when the corresponding adjustments of two consecutive iterations are the same.

5.1.1 k-means Clustering

k-means (also known as c-means) clustering is the best known clustering method [81]. It consists of a sequence of iterative-update rules. The algorithm calculates a cluster center as the mean of the samples belonging to the same cluster as

$$Y_\alpha = \frac{1}{n_\alpha} \sum_{j=1, l_j=\alpha}^{n} S_j, \quad \alpha = 1,\dots,k, \tag{5.1}$$

where S_j, j=1,…,n is the given spectra, Y_α, α=1,…,k is a set of clustering centers, n_α corresponds to a number of elements belonging to the α^{th} cluster, and l_j, j=1,…,n is the indexes of clustering which l_j=α if S_j belongs to the α^{th} cluster. Then the clusters are updated by the minimum of RMSE over the clustering centers and given spectra. For the given spectra S and k – number of clustering, a k-means algorithm follows:

Algorithm 5.1:

Initialize	Y_α = random, α=1,…,k;
	for j=1,…,n
Assign	if ($\| S_j - Y_\alpha \|^2$ is minimal for α=1,…,k)
	then l_j=α;
	do
Remember	$Y_\alpha^{old} = Y_\alpha$, α=1,…,k;
Calculate	Y_α, α=1,…,k, according (5.1)
	for j=1,…,n
Assign	if ($\| S_j - Y_\alpha \|^2$ is minimal α=1,…,k)
	then l_j=α;
Repeat	until ($Y_\alpha^{old} = = Y_\alpha$, α=1,…,k)

The output of the method is a set of the final cluster centers Y_α, α=1,…,k and l_j, j=1,…,n – indexes of clustering to represent which cluster the j^{th} sample belongs to.

5.1.2 Subspace Clustering

A more suitable clustering algorithm for the PCA application was proposed by Parkkinen et al. [84]. The method is based on definition of a projection measure between a subspace and sample spectrum. This measure is defined as the projection length of the sample spectrum s onto the subspace L, which in the case of one-dimensional subspacing is equal to a scalar product between spectrum s and normalized vector ℓ as follows:

$$P_s(\ell) = \frac{< s, \ell >}{\| \ell \|^2}, \tag{5.2}$$

where s is the sample spectrum and ℓ is the one-dimensional basis of the subspace L, and $\|.\|^2$ is the square Euclidean norm.

The iterative-update rules are the same as k-means. The algorithm calculates a cluster center as the first principal component of a spectra S^α, j=1,…,k, where S^α is the spectra composed of the samples belonging to the cluster α defined as the cluster table. It then updates the cluster items by the maximum projection length (5.2).

For the given spectra *S*, the subspace clustering algorithm is as follows:

Algorithm 5.2:

Initialize	$\ell_\alpha = random$, $S^\alpha = \varnothing$, $\alpha=1,\ldots,k$;
Assign	for $j=1,\ldots,n$
	if ($P_{S_j}(\ell_\alpha)$ is maximal for $\alpha=1,\ldots,k$)
	then $l_j=\alpha$;
	do
Remember	$\ell_\alpha^{old} = \ell_\alpha$, $S^\alpha = \varnothing$, $\alpha=1,\ldots,k$;
Form	for $j=1,\ldots,n$
	for $\alpha=1,\ldots,k$
	if ($l_j == \alpha$)
	then $S^\alpha = [S^\alpha, S_j]$;
Calculate	ℓ_α, $\alpha=1,\ldots,k$; as the first Component of spectra S^α from cluster α
Assign	for $j=1,\ldots,n$
	if ($P_{S_j}(\ell_\alpha)$ is maximal $\alpha=1,\ldots,k$)
	then $l_j=\alpha$;
Repeat	until ($\ell_\alpha^{old} == \ell_\alpha$, $\alpha=1,\ldots,k$)

The output of the method is a set of the final cluster centers ℓ_α, $\alpha=1,\ldots,k$ or subspace bases and l_j, $j=1,\ldots,n$ – indexes of clustering to represent which cluster the j^{th} sample belongs to.

Subspace clustering finds clusters as elements distributed along cones (subspace axis) [84]. Although the tip of a cone can only go through the point of origin, it has been hypothesized to decrease the transformation losses. Figure 5.1 presents an example of k-means and subspace clustering applied to the same data set.

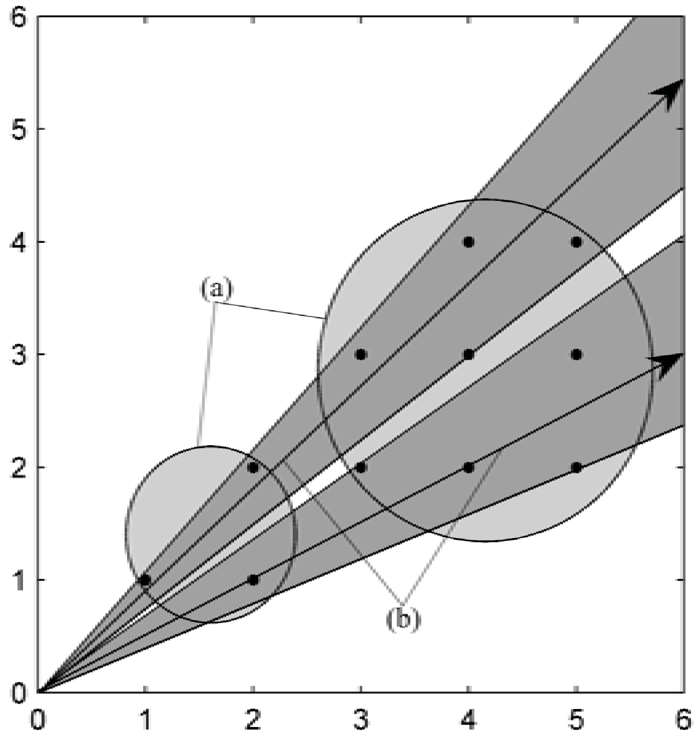

Figure 5.1 *Example of clustering, (a) k-means method, (b) subspace clustering method.*

5.2 PROPOSED COMPRESSION METHOD

Three main specifications for digital image archive compression are considered in this study. First, the time taken by compression is not as significant as the decompression period. Second, the quality of the reconstructed image must be flexible according to the application. The image can be accurately compressed for a reasonably long storage time. Finally, the size of compressed images is aimed at storing as many images as possible because digital archives are characterized by a huge number of processed images.

We hypothesize a lossy compression approach aiming to be most suitable for an application in a historical archive system.

The proposed method consists of a number of sequential steps presented in Figure 5.2. An original image consists of pixels with similar colors. First, the sets of these pixels can be found by clustering performed in the original spectral image or in CIE L*a*b* representation of the original spectra. Next, the original image is transformed to a cluster table where each cluster consists of a single spectrum from the original image. Then each set of spectra belonging to one cluster is transformed by PCA. Finally, the compressed image consists only of the cluster table and components of spectra reduction.

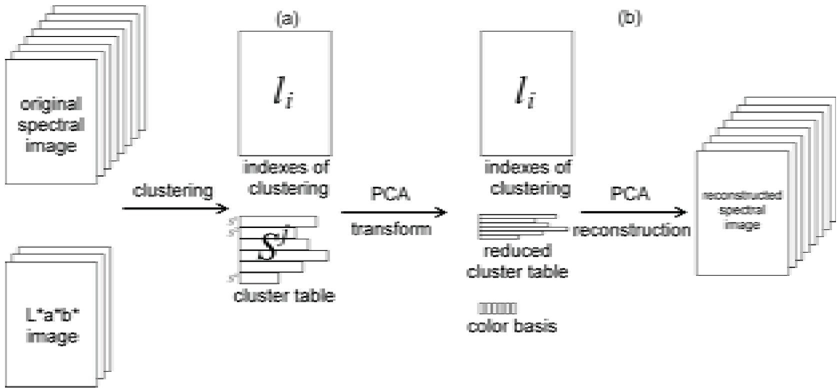

Figure 5.2 Proposed compression technique (a) compression; (b) decompression.

It was shown in [P2] that the clustering performance in CIE L*a*b* space gives a number of benefits. The small size of CIE L*a*b* significantly reduces the CPU time of clustering. Moreover, compression based on CIE L*a*b* clustering represents smaller visual losses then the same compression based on clustering in spectral space. The human visual system is not sensitive enough to recognize small changes in components of color spectra [85]. It allows applying space transformation and “forget about” the least correlated components of the color spectra.

To find spectra sets which are better suited to the PCA application, another clustering technique named subspace clustering was applied in this method [84]. Subspace clustering finds clusters as elements distributed along cones (subspace axis). Although the tip of a cone can only go through the point of origin, it was hypothesized to decrease the transformation losses. Because the clustering is iterative, the proposed method cannot be used for real-time applications like data communication or remote sensing. However, it seems to be best for applications where decompression time and decompressed image quality are more important than compression (e.g. a digital image archive system or web browsing).

6 Retrieval

Due to an increasing amount of digital images, digital image archives require robust retrieval methods that are able to find images in the archive by relevant query [36]. Many methods have been developed in recent years. They are mostly based on the distance between sequential characteristics of the digital image called image features. There are two main classes of image features. The first class concerns the shape of the image content, e.g. LBP [86] and GLCM [87], and the second class concerns the color, e.g. color histogram [88], blob histogram [89], color correlogram [90], and MPEG-7 [91]. Section 6.1 introduces two image features which used in the area of image retrieval: image analysis and pattern recognition.

Spectral image archive systems are characterized by a huge amount of required memory [92]. Spectral images take up a lot of memory even in compressed format. Due to the increasing importance of spectral imaging, spectral image archive systems have become increasingly popular in the last years. However, this area has not been studied yet. Most acquisition, compression and retrieval methods known nowadays are for gray-scale or three chromatic (e.g. RGB) imaging and are not suitable for spectral color usage.

Spectral image indexing retrieval methods have been studied by several authors in the last years [93] [94] [95] [96]. Most studies are based on similarity measurement between spectral image features extracted by spectra reduction methods e.g. principal component analysis (PCA) [7], self-organizing map (SOM) [56], independent component analysis (ICA) [97], and factor analysis (FA) [98]. We propose a new spectral color features extraction technique in [P5]. It is based on non-negative tensor factorization (NTF) and showed good results during the test set. The main benefit of these features is that due to non-negativity they can be implemented optically. The method is presented schematically in Section 6.2.

6.1 IMAGE FEATURES

6.1.1 Color Histogram

The probability density function of the image color or color histogram is widely used for image indexing and retrieval [99]. Comparing with the shape of the image content, the colors of the pixels in the image provide additional information which is used in many pattern recognition and image analysis applications. The color histogram describes the global color distribution in an image. It is obtained by quantization of the color space by the number of equal sized colors and counting the number of pixels belonging into each quantized color [100]. These numbers are further normalized by the total number of pixels in the image. An image color histogram is calculated as

$$h(i) = P(i) = \frac{n_i}{n}, \tag{6.1}$$

where $P(i)$ represents the probability of the i^{th} color, n_i is the number of pixels with the i^{th} color, and n is the total number of pixels in the image.

The color histogram is robust to translation of object and rotation about the viewing axis; it does not include any spatial information. The retrieval method is based on similarity measures proposed before, i.e. RMSE (3.23), GFC (3.24) or PSNR (3.25).

6.1.2 Local Binary Pattern

The Local Binary Pattern (LBP) approach [85] is a spatial filtering method which characterizes the texture properties by means of spatial organization of the neighborhoods. The LBP operator consists of a 3×3 neighborhood, which is thresholded by the value of the centering pixel. The thresholded neighborhood is then multiplied by the corresponding binomial weights and the LBP number varies from 0 to 255. LBP is invariant against any monotonic gray scale transformation, and rotation invariance can be achieved by rotating binomial weights [101]. An example of a calculation of an LBP is shown in Figure 6.1.

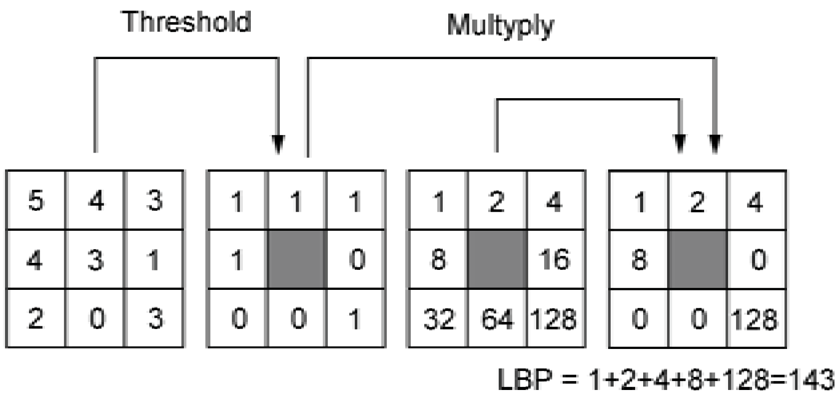

Figure6.1 *Example of a calculation of an LBP.*

6.2 PROPOSED METHOD

A new color based method for spectral image database search is proposed in [P5]. It is based on a similarity measure between spectral image color features. It was supposed that the third component of the Non-negative Tensor Factorization (which is corresponds to the spectral domain) holds the most significant spectral color information suitable for database search. The method was compared with the convenient spectral data analysis technique i.e. Principal Component Analysis.

Non-negative Tensor Factorization (NTF) is a new technique. It represents an original 3D non-negative matrix as tensor multiplication of non-negative bases. The non-negative basis for data description is useful for two reasons. First, the approach is natural since many measuring devices output only non-negative values. Secondly, non-negative filters can be physically implemented. Thus, many possibilities exist for the non-negative bases application. They include feature extraction in image databases, band selection in spectral imaging, and even image compression. The computational complexity of NTF is more complicated than that of PCA. But a new way of NTF with a multiresolution approach is aimed to accelerate the time complexity of the features extraction.

The search method consists of two steps, as presented in Figure 6.2. The first step is feature extraction using one of the proposed methods, e.g. NTF or PCA. For NTF, each spectral image was applied as a 3D non-negative matrix. Bases u, v, and w were obtained using the multiresolution NTF algorithm introduced in Section 3.3. The non-negative basis for the spectral domain (normalized w) defines the spectral image feature. For PCA, each spectrum vector from a spectral image was stored in 2D matrix row wise order. Then, according to the PCA theory, an autocorrelation matrix in a special content was calculated for each spectral image matrix. An orthogonal basis that consists of ordered eigenvectors of the autocorrelation matrix defines the spectral image feature. The second step is measuring the similarly between the extracted features.

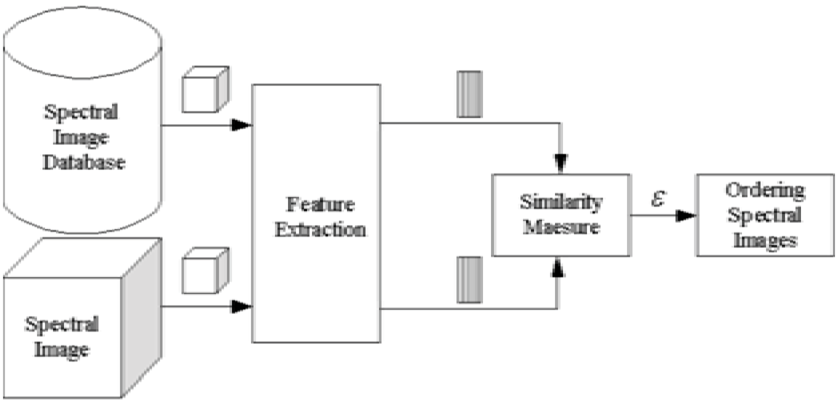

Figure 6.2 *Spectral image database search process.*

.

The similarity between spectral image features was calculated in this study using RMSE (3.23), GFC (3.24) and

PSNR (3.25). However, due to the random initialization, NTF produces different ordered bases for the same spectral image. Therefore the similarity measure must be order independent. To find the similarity between two bases we calculated the similarity between all possible combinations of vectors in the bases. The best value (minimum for RMSE, maximum for GFC and PSNR) was defined as the result.

7 Experiments and Results

Most of the suggestions proposed during the study were empirically proved by experiments. The experiments were performed on PC and Matlab [102] script language and C language were used as the main tools. The sample spectra and spectral images were taken from different sources, e.g. InFotonics [103], AVIRIS [104], CBCL [105], and the University of Bristol [106]. The results of the experiments were published in six international conferences, which the current thesis is based on. From there we are able to conclude the following.

A compression technique most suitable for an application in a historical archive system was proposed in [P2]. The experiments showed the following. Subspace clustering is more suitable for a PCA application than convenient k-means. Due to slow clustering performance, compression takes time. Decompression is fast and the quality of the decompressed image is suitable for a historical image archive. We have obtained the lowest $\Delta E = 2$, in the case of subspace clustering in CIE L*a*b* and the lowest $\varepsilon_{RMSE} = 0.063$ in the case of subspace clustering in spectral space. The clustering number mostly affects the computation time but not the compression ratio. From this it follows that the quality of the decompressed image can be improved with a small decrease in compression ratio. The error measure depends on the space where clustering is performed. ΔE is lower if clustering is applied in CIE L*a*b*.

The concept of NTF acceleration using a multiresolution approach and sampling was proposed and comparably proved in studies [P3] and [P4]. The experiments show that the proposed approach is from 2 to 10 times faster than the original computation. It was also shown that preprocessing is applicable for low k, $k \leq 8$, with respect to the data size used in the experiments.

A color based spectral image retrieval algorithm based on similarity measures between spectra color features is proposed in [P5]. We defined NTF and PCA bases, obtained from image spectra, as the representative characteristics of the image colors (i.e. image features). A new technique of similarity measurement between spectral bases was proposed. It assumes that NTF returns the basis vectors in a random order, as opposed to PCA. The proposed method was implemented and tested on 107 spectral images. To find the most appropriate features and a similarity measure for those features, the method was tested using PSNR, GFC and Euclidean distance. An NMF basis within PSNR was found to be the best match.

We have calculated color filters for five different spectrums in [P6] to evaluate the effect of different light sources on the reconstruction error. The obtained results show that the reconstruction bases are strongly affected by the light source. The properties of the applied light sources are clearly reflected in the corresponding bases. Smooth lights give smooth bases and peaks arise in the corresponding bases in the same order. The reconstruction error was calculated using three well-known measures, namely ΔE, GFC and PSNR, to find the reconstruction parameters more accurately.

8 Summary of the Publications

In the first paper [P1], we aim to find relations between mathematical and human methods for grouping images in order to find more possibilities for developing the actual quality of images for different purposes. In this study, we propose two methods. Hierarchical grouping is one of the ways to perform automatic grouping of images. The method is based on hierarchical steps of objects and image features detection (e.g. people, buildings, trees, sky, cars, etc). In the second way, the explanation group images are searched from Self-Organized Maps. Preliminary results are based on psychological tests on humans, MPEG-7 based features of the images and face detection methods. We also show some notes and questions related to this problem and plans for future research.

The proposed study is the first step in digital image archive investigation. Although most of the results are positive, we are faced with a number of problems. That is the main reason why the spectral image archive is considered further.

My part of this study covers the hierarchical steps of image features detection i.e. face detection. My contribution is about 40–50%.

In the second paper [P2], we propose a spectral image compression technique for spectral archives. The technique consists of a combination of color clustering and spectral reduction. Subspace clustering and k-means are applied in various color spaces. Principal Component Analysis (PCA) is used as a spectra reduction technique. The proposed compression method is compared with the spectral image compression method for data communication. All compression methods are compared by two quantitative error rate measures.

The experiments show that the proposed compression technique is the most suitable for archive systems. However, CPU time increases with the number of clustering but the quality of the reconstructed image can be improved by using a higher number of clustering. The phenomena relationship between the space of clustering and the error measure is explained in conclusion. Also a wide research area for improvement is given here.

My part of this study coves algorithm development, implementation and representation. My contribution is about 80–90%.

In the third paper [P3] we show how to accelerate NTF using a multiresolution approach. The large dataset is preprocessed with an integer wavelet transform, and NTF results from the low resolution dataset are utilized in the higher resolution dataset. The paper does not cover aspects of the digital image archive, but it extends the NTF theory, which is used in all three parts of the spectral image archive studied in this thesis.

The experiments show that the multiresolution based speed-up for NTF computation varies in general from 2 to 10 depending on the dataset size and on the number of required basis functions. That is the reason why the proposed acceleration technique is used for further calculations.

My part of this study covers algorithm implementation and representation. My contribution is about 20–30%.

In the fourth paper [P4] we propose sampling methods for the preprocessing phase which enables a faster way to compute the non-negative tensor factorization (NTF). In preprocessing both sampling and interpolation are applied to the original data because the computational complexity depends on the number of bases, i.e. the rank of the factorization, and on the dimensions of the spectral image. Three approaches are compared: direct subsampling, integer wavelet transform, and spectral smoothing. The paper supposes the extension of the NTF theory for more rapid feature extraction.

The experiments have been applied to five spectral images. The results indicate that preprocessing can remarkably reduce the time needed for NTF. From the approaches, the integer wavelet transform shows the best performance from the computational and quality perspectives. The computational load from direct subsampling is the lowest for one iteration, and spectral smoothing is computationally the heaviest.

My part of this study covers algorithm implementation and manuscript writing. My contribution is about 40–50%.

In the fifth paper [P5] we propose a technique for color based retrieval from a spectral image database. The technique is based on a similarity measure between spectral image features extracted by a spectral reconstructed method. Non-negative tensor factorization (NTF) and principal component analysis (PCA) are applied in a spectral image domain for color feature extraction. The calculations are performed by using multiresolution approach proposed in [P3] and [P4].

The proposed method is implemented and tested with a spectral image database. The images from the database are ordered according to the similarity between them and the tested image. Three similarity measures were applied in the two spectral image feature spaces. The results of the experiments are visually presented in the paper. The best combination of the spectral image feature and similarity measure in our opinion is NTF and PSNR correspondently. Further work will be proposed.

My part of this study covers algorithm development, implementation and manuscript writing and presentation. My contribution is about 80–90%.

In the sixth paper [P6] we found illuminant dependence of Principal Component Analysis (PCA), Non-negative Matrix Factorization (NMF) and Non-negative Tensor Factorization (NTF) in spectral color imaging. All these methods are applied as dimension reduction methods in the color spectrum domain. The effect of light sources on the quality of the reconstructed spectrum is investigated.

Five reflectance spectra sets from different sources were used in tests. Four light source spectrums with various shapes were applied for light source simulation. We evaluate the reconstruction spectrum by quality and error measures including ΔE, GFC and PSNR. The obtained results show that the non-negative basis of NTF and NMF are more suitable for optical implementation than PCA. Because of the similarity of the reconstruction error and the fact that the best reconstruction was obtained under peaky light sources, we can build an LED based acquisition system prototyped in this thesis.

My part of this study covers algorithm development, implementation and manuscript writing and presentation. My contribution is about 80–90%.

9 Conclusions

The dissertation is a compendium of the publications collected during the study of fundamental spectral image archiving components i.e. the processes of image acquisition, compression and retrieval. It was supposed that PCA, NMF and NTF (defined as reconstruction methods in this thesis) are suitable to be applied to all the components of the spectral image archive, and future research has been proposed for each of them. The reconstruction methods were applied in ways of data reduction, feature extraction and color spectra reconstruction. The results of experiments were published with the following conclusions.

PCA is a convenient method, and its importance for the spectral imaging area has been shown by several authors before. It has been widely used for spectra reduction due to the high correlation of color spectra components. The dissertation based on the mentioned phenomena introduces a new compression method which is suitable for spectral image archives. It was also supposed that the compression technique can be applied by improving the introduced clustering method according to a spectral image's source and application.

It was shown that the non-negative basis gives a number of benefits compared to the orthogonal one. It can be implemented optically with approximately the same reconstruction error as with the orthogonal, but the number of required measurements is half as many. Based on these phenomena, a spectral acquisition system based on color spectra reconstruction was hypothesized. The system considers light source simulation. The light source spectra are calculated using one of the non-negative spatial methods instead of an orthogonal one. Moreover, the features obtained by NTF show better relevance for spectral image retrieval. The spectral image retrieval method was proposed during this study. The method finds similar images in the database according to the non-negative bases obtained by NTF instead of using irrelevant features which are more convenient for grayscale and trichromatic image retrieval.

The CPU time required for bases calculation is the biggest weakness of the non-negative methods introduced in the dissertation. Although the multiresolution approach aiming to reduce calculation time introduced in the thesis shows significant improvements, I believe it is still possible to find faster and more efficient methods for non-negative matrix factorization.

References

[1] G. Sharma, *Digital Color Imaging handbook*, Webster, New York, 2002.

[2] P.C. Lauterbur, "Image Formation by Induced Local Interactions: Examples of Employing Nuclear Magnetic Resonance," *Nature*, vol. 242, pp. 190–191, 1973.

[3] Vallebona, "Nouvélle méthode roentgenstratigraphique," *Schweizerische medizinische Wochenschrift*, vol. 78(14), pp. 341, 1948.

[4] W. C. Röntgen, "On a New Kind of Rays," *Nature*, vol. 53, pp. 274–276, 1896.

[5] R. C. Gonzalez, R. E. Woods, *Digital Image Processing*, third edition, Pearson Prentice Hall, New Jersey, 2008.

[6] K. Martinez, J. Cupitt, D. Saunders, R. Pilay, "Ten Years of Art Imaging Research," *Proceedings of the IEEE*, vol. 90(1), pp. 28-41, 2002.

[7] T. Jolliffe, *Principal Component Analysis*, Springer-Verlag, New York, 1986.

[8] D. Lee, H. Seung, "Learning the Parts of Objects by Nonnegative Matrix Factorization," *Nature*, vol. 401, pp. 788–791, 1999.

[9] Shashua, T. Hazan, "Non-Negative Tensor Factorization with Applications to Statistics and Computer Vision," *Proceedings of International Conference on Machine Learning, ICML*, pp. 793-800, 2005.

[10] P. K. Kaiser, R. M. Boynton, *Human Color Vision*, 2nd edition, Optical Society of America, Washington DC, 1996.

[11] J. Gage, *Color and Meaning: Art, Science and Symbolism*, University of California Press, 2000.

[12] N. Ohta, A. Robertson, *Colorimetry Fundamentals and Applications*, Wiley, 2005.

[13] W.B. Marks, W. H. Dobelle, E. F. MacNichol, "Visual pigments of single primate cones," *Science*, vol. 143, pp. 1181-1183, 1964.

[14] *CIE Proceedings 1931*, Cambridge University Press, Cambridge, UK, 1932.

[15] W. G. Wright, "A Re-determination of the Trichromatic Coefficients of the Spectral Colours," *Transactions of the Optical Society*, vol. 30, pp. 141-164, 1929.

[16] J. Guild, "The Colorimetric Properties of the Spectrum," *Philosophical Transactions of the Royal Society of London*, vol. 230, pp. 149-187, 1931.

[17] J. Schanda, Colorimetry: understanding the CIE system, John Wiley & Sons, 2007.

[18] R. Robertson, "The CIE 1976 Color-difference formulate," *Color Research and Applications,* vol. 2, pp. 7-11, 1977.

[19] G. Sharma, *Digital Color Imaging handbook*, CRC Press, 2003.

[20] J. Lehtonen, J. Parkkinen, T. Jääskeläinen, "Optimal Sampling of Color Spectra," *Journal of the Optical Society of America*, vol. 23(12), pp. 2983-2988, 2006.

[21] T. Jetsu, P. Herzog, T. Jääskeläinen, J. Parkkinen, "Standardization of Spectral Image Formats," *Proceedings, 7th International Conference on Pattern Recognition and Image Analysis*, vol. 15(3), pp. 618-620, 2005.

[22] http://www.multispectral.org/, August 24, 2009.

[23] P. Herzog, *MUSP Multispectral Image File Format, Version 1.4*, Color AIXperts GmbH, Aachen, 2003.

[24] *Natural Vision Data File Format Specification, Version 2.0s*, Akasaka Natural Vision Research Center, National Institute of Information and Communications Technology, 2003.

[25] D. S. Taubman, M. W. Marcellin, *JPEG2000: Image Compression Fundamentals, Standards and Practice*, Kluwer Academic, Dordrecht, 2002.

[26] TIFF 6.0 Specification (Adobe System Incorporated, Adobe Developers Association, 1992), http://partners.adobe.com/asn/developer/PDFS/TN/TIFF6.pdf, August 24, 2009.

[27] DHF5 (The National Center for Supercomputing Applications, University of Illinois, 2003); HDF5-A new Generation of HDF (Introduction to HDF5, HDF5 User's Guide), 2003.

[28] V. Naydenova, G. Jelev, "Forest dynamics study using aerial photos and satellite images with very high spatial resolution," *Proceedings of Recent Advances in Space Technologies, 2009. RAST '09*, pp. 344-348, 2009.

[29] R. Singh, M. Vatsa, A. Noore, "Multiclass mv-granular soft support vector machine: A case study in dynamic classifier selection for multispectral face recognition," *Proceedings 19th International Conference of Pattern Recognition, ICPR 2008*, pp.1-4, 2008.

[30] O. Kohonen, J. Parkkinen, T. Jääskeläinen, "Databases for Spectral Color Science," *Color Research and Application*, vol. 31(5), pp. 381-390, 2006.

[31] R. Sandau, *Digital Airborne Camera Introduction and Technology*, DLR, Berlin, 2010.

[32] R. D. Fiete, *Modeling the Imaging Chain of Digital Cameras*, SPIE Press, 2010

[33] E. Bayer, "Color Imaging Array," US Patent No. 3971065, 1976.

[34] J. Friedman, *History of Color Photography*, Focal Press, New York, 1969.

[35] Kaarna, "Companding and PCA Compression of Spectrum Sets," *Proceedings Geoscience and Remote Sensing Symposium, IGARSS '05*, vol. 1, pp. 124-127, 2005.

[36] F. Long, H. Zhang, D. Feng, "Fundamentals of Content-Based Image Retrieval," *Multimedia Information Retrieval and Management- Technological Fundamentals and Applications, Springer*, 2003.

[37] Cichocki, M. Morup, P. Smaragdis, W. Wang, R. Zdunek, "Advances in Nonnegative Matrix and Tensor Factorization (Editorial)," *Computational Intelligence and Neuroscience*, vol. 2008(2), 2008.

[38] K. Pearson, "On Lines and Planes of Closest Fit to Systems of Points in Space," *Philosophical Magazine*, vol. 2, pp. 559–572, 1901.

[39] S.A. Robila, L.G. Maciak, "Considerations on Parallelizing Nonnegative Matrix Factorization for Hyperspectral Data Unmixing," *Proceedings of Geoscience and Remote Sensing Letters*, vol. 6, pp. 57-61, 2009.

[40] J. S. Lee, D. D. Lee, C. Seungjin, S. P. Kwang, D. S. Lee, "Non-negative Matrix Factorization of Dynamic Images in Nuclear Medicine," *Proceedings of Nuclear Science Symposium Conference Record*, vol. 4, pp. 2027-2030, 2001.
[41] P. O. Hoyer, "Non-negative Matrix Factorization with Sparseness Constrains," *Journal of Machine learning Research*, vol. 5, pp. 1457-1469, 2004.
[42] D. Lee, H. S. Seung, "Algorithms for Non-negative Matrix Factorization," *Proceedings of Neural Information Processing Systems*, pp. 556–562, 2000.
[43] T. Hazan, S. Polak, A. Shashua, "Sparse Image Coding Using a 3D Non-Negative Tensor Factorization," *Proceedings of International Conference on Computer Vision, ICCV*, pp. 50- 57, 2005.
[44] Shashua, R. Zass, T. Hazan, "Multi-way Clustering Using Super-symmetric Non-negative Tensor Factorization," *Proceedings of the European Conference on Computer Vision, ECCV*, pp. 595-608, 2006.
[45] S. Mallat, *A wavelet tour of signal processing*, San Diego (CA) Academic Press, 1999.
[46] Daubechies, *Ten Lectures on Wavelets CBMS-NSF. Regional Conference Series in Applied Mathematics*, Philadelphia, 1992.
[47] V. K. Haar, H.-E. Reinfelder, "A Comparison of Reversible Methods for Data Compression," *Proceedings of SPIE, Medical Imaging IV*, vol. 1233, pp. 354-365, 1990.
[48] Webb, *Statistical Pattern Recognition*, Wiley & Sons Inc., Chichester, UK, 2004.
[49] Avcibas, B. Sankur, K. Sayood, "Statistical Evaluation of Image Quality Measures," *Journal of Electronic Imaging*, vol. 11(2), pp. 206–223, 2002.
[50] Girod, "What's wrong with Mean-Squared Error," *Digital Images and Human Vision*, pp. 207-220, 1993.
[51] J. Hernández-Andrés, J. Romero, R. L. Lee, "Colorimetric and Spectroradiometric Characteristics of Narrow-field-of-view Clear Skylight in Granada, Spain," *Journal of the Optical Society of America*, vol. 18(2), pp. 412-420, 2001.

[52] Salomon, G. Motta, and D. Bryant, *Data Compression: The Complete Reference, 4rd edition*, Springer, 2007.

[53] R. A. Johnson, *Advanced Euclidean Geometry*, Dover Publications, 2007.

[54] Nippolainen, A. Kamshilin, "Computer Controlled Set of Light-Emitting Diodes for 2d Spectral Analysis," *Processdings of 4th European Conference on Colour in Graphics, Imaging and Vision, CGIV*, pp. 481-483, 2008.

[55] J. Hallikainen, J. Parkkinen, T. Jääskeläinen, "Color Image Processing with AOTF," *Proceedings of the 6th Scandinavian Conference on Image Analysis*, pp. 294-300, 1989.

[56] H. Laamanen, K. Miyata, M. Hauta-Kasari, J. Parkkinen, T. Jääskeläinen, "Imaging Spectrograph Based Spectral Imaging System," *Proceedings of Second European Conference on Color in Graphics, Imaging, and Vision, and Sixth International Symposium on Multispectral Color Science*, pp. 427-430, 2004.

[57] M. J. Vrhel, R. Gershon, L. Iwan, "The Measurement and Analysis of Object Reflectance Spectra," *Color Research and Application*, vol. 19(1), pp. 4-9, 1994.

[58] J. Parkkinen, J. Hallikainen, T. Jääskeläinen, "Characteristic Spectra of Munsell Colors," *Journal of the Optical Society of America*, vol. 6(2), pp. 318-322, 1989.

[59] M. Hauta-Kasari, K Miyazawa, S. Toyooka, J. Parkkinen, "A Prototype of the Spectral Vision System," *Proceedings of the 11th Scandinavian Conference on Image Analysis*, pp. 79-86, 1999.

[60] S. Tominaga, "Multichannel Vision System for Estimating Surface and Illumination Functions," *Journal of the Optical Society of America*, vol. 13(11), pp. 2163–2173, 1996.

[61] S. Baronti, A. Casini, F. Lotti, S. Porcinai, "Multispectral Imaging System for the Mapping of Pigments in Works of Art by Use of Principal-Component Analysis," *Journal of Applied Optics*, vol. 10(8), pp. 1299-1309, 1998.

[62] H. Haneishi, T. Hasegawa, N. Tsumura, Y. Miyake, "Design of Color Filters for Recording Art Works," *Processdings of IS&T's 50th Annual Conference*, pp. 369-372, 1997.

[63] R. Lenz, M. Osterberg, J. Hiltunen, T. Jääskeläinen, J. Parkkinen, "Unsupervised Filtering of Color Spectra," *Journal of the Optical Society of America*, vol. 13(7), pp. 1315-1324, 1996.

[64] H. Haneshi, T. Hasegawa, A Hosoi, Yokoyama, N. Tsumura, y. Miyake, "System Design for Accurately Estimating the Spectral Reflectance of Art Paintings," *Journal of the Applied* Optics, vol. 39(35), pp. 6621-6632, 2000.

[65] Schmitt, H. Brettel and J. Y. Hardeberg, "Multispectral imaging development at ENST," *Proceedings of the International Symposium of Multispectral Imaging and Color Reproduction for Digital Archive*, pp. 50-57, 1999.

[66] M. J. Vrhel, R. Gershon, L. S. Iwan, "Measurement and Analysis of Object Reflectance Spectra," *Journal of the Color Research and Application*, vol. 9, pp. 4–9, 1994.

[67] H. Haneishi, T. Hasegawa, A. Hosoi, Y. Yokoyama, N. Tsumura, Y. Miyake, "System Design for Accurately Estimating the Spectral Reflectance of Art Paintings," *Journal of the Applied Optics*, vol. 39(35), pp. 6621-6632, 2000.

[68] N. Tsumura, H. Haneishi, Y. Miyake, "Estimation of Spectral Reflectance from Multi-band Images by Multiple Regression Analysis," *Journal of the Japanese Journal of Optics*, vol. 27(7), pp. 384-391, 1998.

[69] Kaarna, K. Tamura, S. Nakauchi, "Non-Negative Bases for Spectral Color Sets," *The Second International Workshop on Image Media and its Applications*, 2007.

[70] M. Hauta-Kasari, W. Wang, S. Toyooka, J. Parkkinen, R. Lenz, "Unsupervised Filtering of Munsell Spectra," *Proceedings of the 3rd Asian Conference on Computer Vision*, vol. 1, pp. 248-255, 1998.

[71] Munsell Book of Color. Matte Finish Collection. Munsell Color, Baltimore, USA, 1976.

[72] S. Grossberg, *Studies of the Mind and Brain*, Reidel Press, 1982.

[73] T. Kohonen, *Self-Organization Maps*, Springer-Verlag, 1995.

[74] S. Haykin, *Neural Networks a Comprehensive Foundation*, Macmillan College Publishing Company, 1994.

[75] K. Sayood, *Lossless Compression Handbook*, Academic Press, 2003.

[76] Q. Du, J. E. Fowler, "Hyperspectral Image Compression Using JPEG2000 and Principal Components Analysis," *Proceedings of*

IEEE Geoscience and Remote Sensing Letters, vol. 4(2), pp. 201-205, 2007.

[77] J. Ma, Y. Li, C. Wu, D. Chen, "Adaptive Interference Hyperspectral Image Compression with Spectrum Distortion Control," *Proceedings of Chinese Optics Letters*, vol. 7, pp. 934-937, 2009.

[78] M. Klimesh, A. Kiely, H. Xie, N. Aranki, "Improving 3D Wavelet-Based Compression of Hyperspectral Images," *Proceedings of NASA Tech Briefs, NPO-41381*, vol. 33(3), pp. 7a–8a, 2009.

[79] M. Hauta-Kasari, J. Lehtonen, J. Parkkinen T. Jääskeläinen, "Spectral Image Compression for Data Communications," *Proceedings of Color Imaging: Device-Independent Color, Color Hardcopy, and Graphics Arts VI, Reiner Eschbach, Gabriel G. Marcu, Editors*, vol. 4300, pp. 42-49, 2001.

[80] Song, L. Hu, Y. Feng, "Hyperspectral Image Compression Based on Wavelets and Uniform Directional Filter Banks," Proceedings of WRI World Congress on Computer Science and Information Engineering, CSIE, vol. 5, pp. 129-133, 2009.

[81] Kaarna, P. Zemcik, H. Kälviäinen, J. Parkkinen, "Multispectral Image Compression," *Proceedings of 14th International Conference on Pattern Recognition*, vol. 11, pp. 1264-1267, 1998.

[82] Kaarna, J. Parkkinen, "Wavelet Compression of Multispectral Images," *Proceedings of the IASTED International Conference on Computer Graphics and Imaging, CGIM 98*, pp. 142-145, 1998.

[83] R. O. Duda, P. E. Hart, D. G. Stork, *Pattern Classification*. 2nd edition, Wiley&Sons, 2001.

[84] J. Parkkinen, E. Oja, "On Subspace Clustering," *Proceedings of 7th International Conference of Pattern Recognition*, vol. 2, pp. 692-695, 1984.

[85] P. G. J. Barten, *Hyman Eye and Its Effects on Image Quality*, SPIE Optical Engineering Press, 1999.

[86] T. Ojala, M. Pietikainen, D. Harwood, "A Comparative Study of Texture Measures with Classification Based on Feature Distributions," *Pattern Recognition*, vol. 29(1), pp. 51-59, 1996.

[87] R. M. Haralick, K. Shunmugam, J. Dinstein, "Textual Features for Image Classification," *Proceedings of IEEE Transactions on System. Man and Cybernetics*, vol. 3(6), pp. 610-621, 1973.

[88] Y. Deng, B. S. Manjunath, C. Kenney, M.S. Moore, H. Shin, "An Efficient Color Representation for Image Retrieval," *Proceedings of IEEE Transactions on Image Process*, vol. 10, pp. 140-147, 2001.

[89] R.J. Qian, P.L.J. van Beek, M.I. Sezan, "Image Retrieval Using Blob Histograms," *Proceedings of IEEE, International Conference on Multimedia and Expo*, vol. 4261, pp. 125-128, 2000.

[90] J. Huang, S. R. Kumar, M. Mitra, W.-J. Zhu, R. Zabih, "Image Indexing Using Color Correlograms," *Proceedings of the 1997 Conference on Computer Vision and Pattern Recognition*, p.762-768, 1997.

[91] T. Sikora, "The MPEG-7 Visual Standard for Content Description - An Overview," *Proceedings of the IEEE Trans. on Circuits and Systems for Video Technology*, vol. 11(6), pp. 696-702, 2001.

[92] O. Kohonen, *Retrieval of Databased spectral Images*, PhD Thesis, University of Joensuu, 2007.

[93] M. Hauta-Kasari, K. Miyazawa, J. Parkkinen, T. Jääskeläinen, "Searching Technique in a Spectral Image Database," *Proceedings of the 13th Scandinavian Conference on Image Analysis*, pp. 927-933, 2003.

[94] O. Kohonen, M. Hauta-Kasari, "Retrieval from a Spectral Image Database by Reconstructed Spectral Images and the Combinations of Inner Product Images," *Proceedings of the 9th International Symposium on Multispectral Colour Science and Application*, pp. 67-72, 2007.

[95] M. Soryani, P. Kabiri, H. Shahbazi, "Content Based Multispectral Image Retrieval Using Principal Component Analysis," *Proceedings of the ACM International Conference on Image and Video Retrieval, CIVR2008*, pp. 205-210, 2008.

[96] P. Martinez, P.L. Aguilar, R.M. Perez, A. Plaza, "Systolic SOM Neural Network for Hyperspectral Image Classification, in: Neural Networks and Systolic Array Design, Edited by D. Zhang and S.K. Pal," *World Scientific*, pp. 193-204, 2002.

[97] Hyvärinen, J. Karhunen, E. Oja, *Independent Component Analysis*, Wiley, New-York, 2001.

[98] R. Reyment, K. Joreskog, *Applied Factor Analysis in the Natural Science*, Cambridge University Press, 1996.

[99] Y. Zang, *Semantic-Based Visual Information Retrieval*, IRM Press, 2007.

[100] M. J. Swain, D. H. Ballard, "Color indexing," *International Journal of Computer Vision*, vol. 7(1), pp. 11–32, 1991.

[101] T. Mäenpää, *The Local Binary Pattern Approach to Texture Analysis – Extensions and Applications*, PhD Thesis, University of Oulu, 2003.

[102] MathWorks, http://www.mathworks.com/, May 10, 2010.

[103] InFotonics, http://ifc.joensuu.fi/, May 10, 2010.

[104] AVIRIS, http://aviris.jpl.nasa.gov/, May 10, 2010.

[105] CBCL, http://cbcl.mit.edu/software-datasets/heisele/facerecognition-database.html, May 10, 2010.

[106] University of Bristol, http://www.bristol.ac.uk/, May 10, 2010.

Alexey Andriyashin

Non-negative bases in spectral image archiving

The objective of this study was to show benefits of non-negative methods in spectral image archiving. Processes of an image acquisition, compression and retrieval were considered as fundamental components of a digital image archiving. Principal Component Analysis, Non-negative Matrix Factorization and Non-negative Tensor Factorization were applied as a spectral reconstruction, a spectral reduction and feature extraction methods.

UNIVERSITY OF
EASTERN FINLAND

Publications of the University of Eastern Finland
Dissertations in Forestry and Natural Sciences

isbn: 978-952-61-0568-0
issn: 1798-5676 (pdf)
issnl: 1798-5668